ON

BARYON RESONANCES

P J Litchfield

CERN, Geneva*

Last year at Aix-en-Provence Ian Butterworth compared his review of resonances with a mini-skirt. To continue in the same vein I would compare this review with a striptease. I hope it will be suggestive, but you may be left with the impression that there is something that you have not seen. This is partly due to pressure of space which means that I cannot do justice to all the contributions to the conference, for which I apologise, but also to the tantalising situation in the subject at present where the outer veils have been discarded so that we can see the underlying form and structure of the resonance spectrum but still the ultimate secret is not revealed.

I believe that the last two or three years have shown great advances with the filling of the SU(6) supermultiplets (practically complete multiplets now exist in their S=0 and S=-1 levels for the

$\{56, 0^+\}_{n=0}$, $\{56, 0^+\}_{n=2}$, $\{56, 2^+\}$ and $\{70, 1^-\}$

together with indications of several others) and systematics amongst the supermultiplets themselves are becoming apparent. Also parallel theoretical advances have been made with the detailed calculation of levels in the harmonic oscillator quark model and the Melosh transformation providing a link between current and constituent quarks.

This progress has been made despite a general slackening of interest in low energies amongst experimentalists now that the unexplored delights of the multi-hundred GeV regions are becoming available. It is my impression that though these high energies are very interesting they are not going to tell us anything about the problems we have been investigating for the past 15 years in the regions below 5 GeV and that it would be a pity to abandon these studies now that we seem at last to be approaching a solution.

This review will be divided into five sections. The first three will consider the new results presented on the strangeness +1, 0 and -1 systems respectively. In section 4 I will review the experimental situation of the resonance spectrum and give tables of resonances with their current status and in section 5 I will attempt to assign these states to their SU(6) x O(3) supermultiplets.

1) STRANGENESS +1 (KN) REACTIONS

The I=1, S=+1 elastic phase shifts seem now to be rather well determined below 1 GeV/c and even up to 2 GeV/c the general features of the amplitudes are understood. New data on K^+p elastic differential cross sections is presented in the very low incident momentum region (130 to 755 MeV/c) by Cameron et al. of the BGRT collaboration (953). This confirms that down to the lowest momenta the coulomb-nuclear interference is constructive indicating a negative s-wave phase shift. Figure 1 shows the angular distributions at 145 and 175 MeV/c. The solid line is the fit with constructive coulomb-nuclear interference the dashed with destructive. An analysis up to 755 MeV/c yields the phase shifts shown in Figure 2. Over this range the amplitudes are all purely elastic and the best values for the scattering lengths and effective ranges are

$a_{s1/2} = -0.309 \pm 0.002$fm $\quad r_{s1/2} = 0.32 \pm 0.02$fm

$a_{p1/2} = -0.021 \pm 0.002(\text{fm})^3$ $\quad a_{p3/2} = 0.013 \pm 0.001(\text{fm})^3$

*Address from 1st August 1974, Rutherford Laboratory.

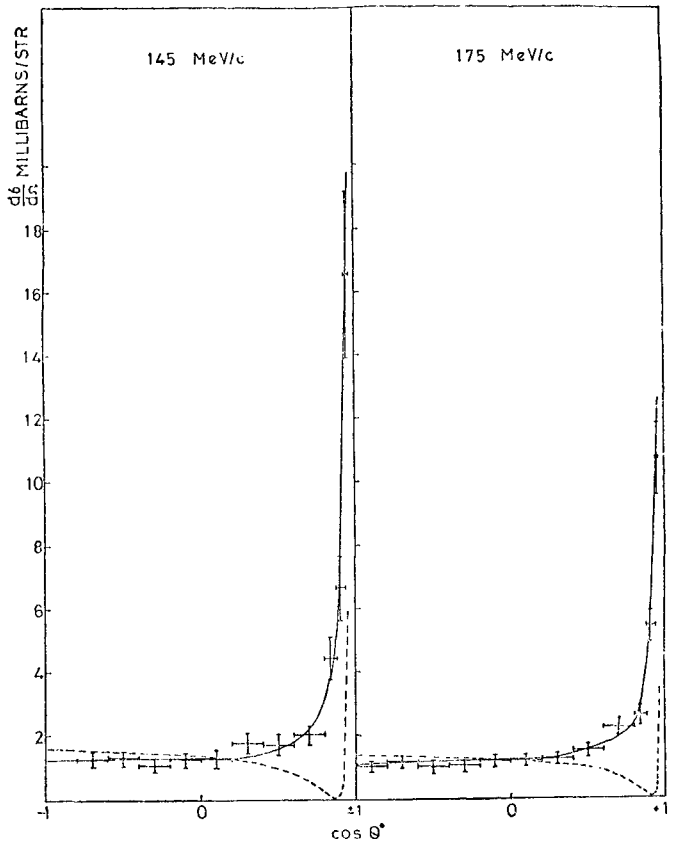

Fig. 1 Angular distributions for $K^+p \to K^+p$ at 145 and 175 MeV/c. The solid lines are fits with a negative s wave phase shift, the dashed lines with a positive s wave phase shift.

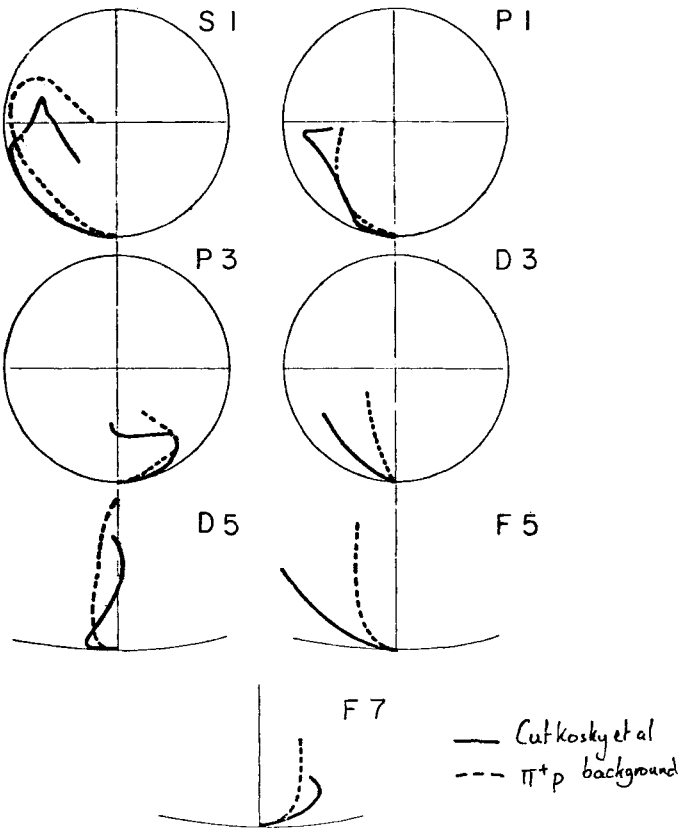

Fig. 3 The solid lines are the K^+p partial waves found by the analysis of Culkosky et al. The dashed lines are the background π^+p amplitudes from Ayed and Barayre[3].

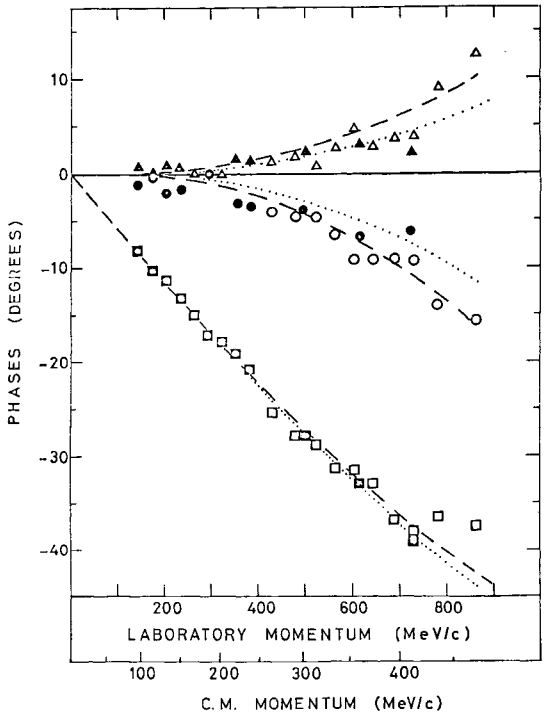

Fig. 2 K^+p phase shifts as a function of energy from Cameron et al. The squares are the $s_{\frac{1}{2}}$, circles $p_{\frac{1}{2}}$ and triangles $p_{\frac{3}{2}}$ phase shifts. The solid lines are the result of an energy dependent analyses and the dotted lines the result of an effective range fit.

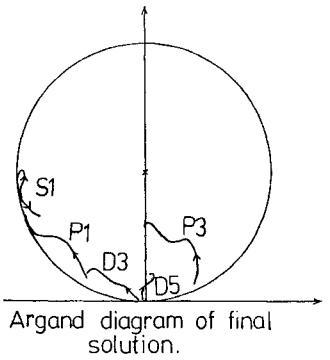

Fig. 4 K^+p partial wave amplitudes from the analysis of Fich et al.

These are generally in good agreement with previous work though the authors state that their errors are probably underestimated.

Above 750 MeV/c two analyses have been presented. The first, covering the region up to 2.5 GeV/c, from Cutkosky et al. (326) has used the ACE procedure[1] for single energy fits combined with partial wave dispersion relations to provide energy smoothing. The amplitudes are shown as the solid lines in Figure 3. The partial waves show strong threshold effects but improved fits to the partial wave dispersion relations were not obtained when explicit resonance poles were added in the s and p waves. The second analysis, covering the region 0.43 to 2.0 GeV/c, by Fich et al. (613) uses fixed t dispersion relations to provide extra theoretical "data". Their resultant amplitudes are shown in Figure 4. Remembering that the energy range of this analysis is considerably less than that of Cutkosky et al. a comparison of the amplitudes shows quite reasonable agreement, at least in general structure. At low momenta they agree reasonably well with Cameron et al. though the p waves are slightly larger.

It has been previously pointed out[2] that the K^+p amplitudes are very similar to the background amplitudes in π^+p after the resonance contribution has been removed. The dashed lines on Figure 3 are the π^+p background amplitudes of Ayed and Bareyre[3]. The agreement is indeed striking. In particular the behaviour of the P3 amplitude which has been intriguingly similar to a resonance loop is approximately reproduced in the π^+p amplitudes reinforcing the general conclusion that the loop is not resonance produced.

The model of Alcock and Cottingham[4] in which the high partial waves are calculated from two and three pion exchange has been remarkably successful in predicting not only the high waves but also the d and p waves. Two papers are presented in which this approach is extended by adding other t- and u- channel exchanges. In the analysis of Cottingham et al. (417) contributions from ε, ρ, ω and A exchanges were added to the calculation of the peripheral partial waves. Using the Birmingham solution of Adams et al. for the S, P and D wave amplitudes, good fits to the differential cross sections and polarisation measurements between 0.9 and 1.5 GeV/c were obtained, (χ^2/number of data points = 906/895) and values for the four coupling constants obtained. Gustafson et al. (614) have applied similar principles to both KN and $\bar{K}N$, $\Lambda\pi$ and $\Sigma\pi$ scattering. Their analysis of KN shows qualitative agreement with the KN phase shift analyses and they would support the resonance interpretation of the P01 phase shift. In the strangeness -1 channels the ω repulsion changes to attraction giving a nett long range attraction in all states. They find general agreement with the dominant resonance structure.

The I=0 KN phase shifts have proved experimentally difficult to evaluate because they have relied on data from K^+n interactions with all the uncertainties involved in deuterium reactions plus the lack of polarisation information. London[5] recently pointed out that they are also accessible through the reaction

$$K_L^o p \rightarrow K_s^o p$$

and that in fact this reaction has powerful advantages over the K^+ reactions studied previously. The amplitude (T) for the above reaction is given by

$$T = \tfrac{1}{4}Z_1 + \tfrac{1}{4}Z_o - \tfrac{1}{2}Y_1$$

where Z_1 and Z_o are the I=1 and I=0 strangeness +1 amplitudes and Y_1 is the I=1 strangeness -1 amplitude. One of the major disadvantages of K^+N partial wave analyses relative to K^-N is the lack of well known reference amplitudes provided by the dominant resonances in K^-N. From the above amplitude it is clear that in K_L^o interactions this lack of resonances in KN is overcome by interferences with the strong

resonances in the Y_1 amplitude. London (135) has repeated the BGRT energy dependent KN analysis including the K_L^o data. The Z_1 and Y_1 amplitudes are taken as known and only the Z_o amplitudes allowed to vary. The three BGRT solutions[6] (A, C and D) were taken as starting values and only solutions close to these in parameter space have been examined. The A and C solutions are probably non resonant whereas the D solution has a strong resonance like loop in P01. Below 1 GeV/c the C and D solutions are similar. Since data below the BGRT analysis is being used (Cho et al (105)) the extrapolation of the BGRT solutions was checked with the solutions of Stenger et al[7] and found to agree. There is an indication that A and C, D are Fermi-Yang ambiguities. Minimisation yielded χ^2/NDF of 2.7, 2.1 and 1.9 respectively for the three solutions compared with 2.2, 2.2 and 1.5 for the fits without the K_L^o data. New solutions A' C' and D' are produced. C' and D' are very little changed from C and D but the S01 and P01 amplitudes of A' have changed appreciably. Figures 5, 6 and 7 show the fits to the $K_L^o p$ total cross section, the $K_L^o p \to K_S^o p$ differential cross section of Cho et al (105) at 550 MeV/c and the recoil proton polarisation in K^+n charge exchange at 600 MeV/c[8].

In all three cases A' is rather strongly disfavoured but solutions C' and D' cannot be separated. However most of the K_L^o differential cross section data, which will provide the best separation, is below 1 GeV/c where C' and D' are very similar. The Argand diagrams of C' and D' are shown in Figure 8. Clearly statistically the fits are poor but this is probably due to the fixing of the Z_1 and Y_1 amplitudes which are not well known, particularly at high energies and in the low Y_1 amplitudes. However the technique seems very promising and when the new K_L^o data at present being analysed[9,10], becomes available it is clear that a complete combined partial wave analysis of

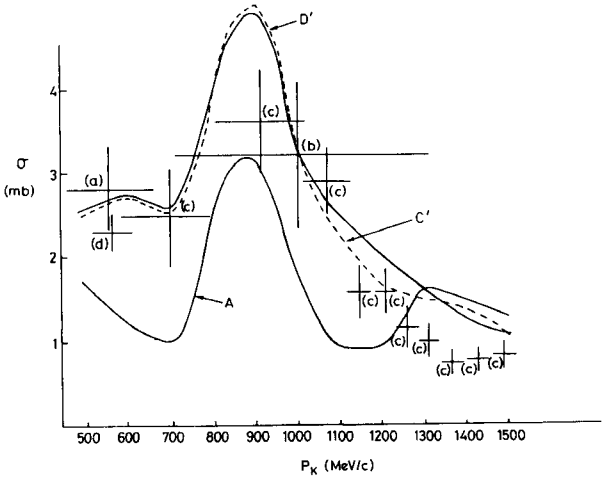

Fig. 5 Measurements of the total cross section for $K_L^o p \to K_S^o p$ plotted as a function of incident beam momentum. The curves are the predictions of the three fits described in the text.

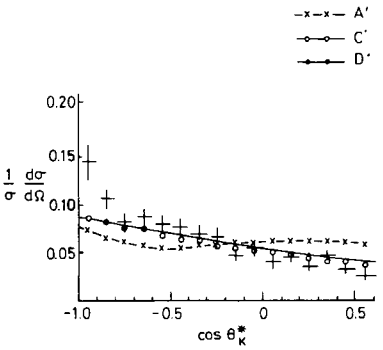

Fig. 6 Normalised differential cross section for $K_L^o p \to K_S^o p$ at 550 MeV/c from Cho et al.[105] together with the prediction of the three fits.

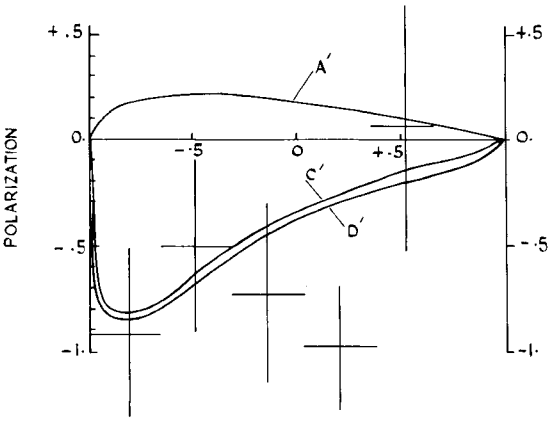

Fig. 7 Recoil proton polarisation in the K^+n change exchange scattering at 600 MeV/c compared to the predictions of the three fits.

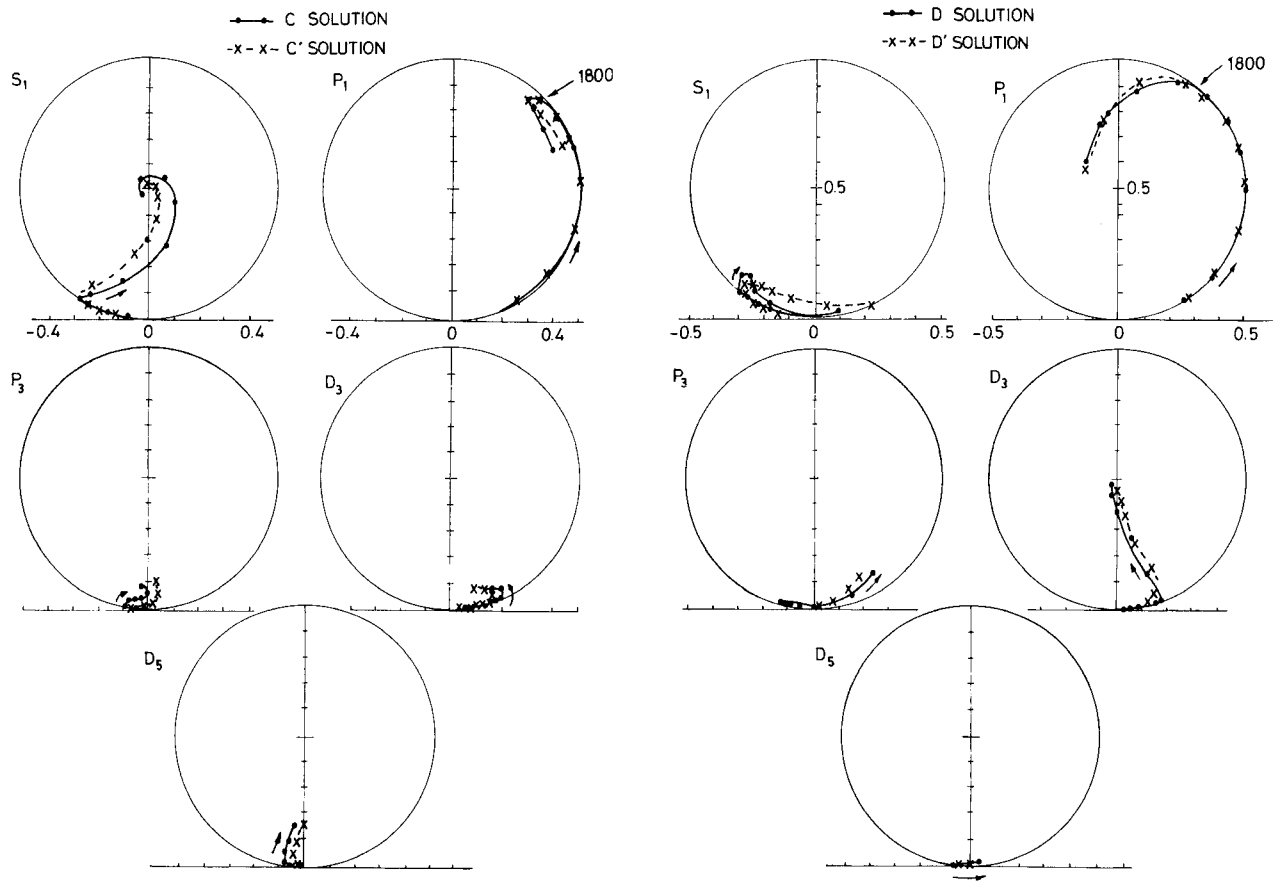

Fig. 8 The argand diagram of the original solutions C and D (solid line) compared with the solution after fitting the K_L^o data (C' and D', dashed lines).

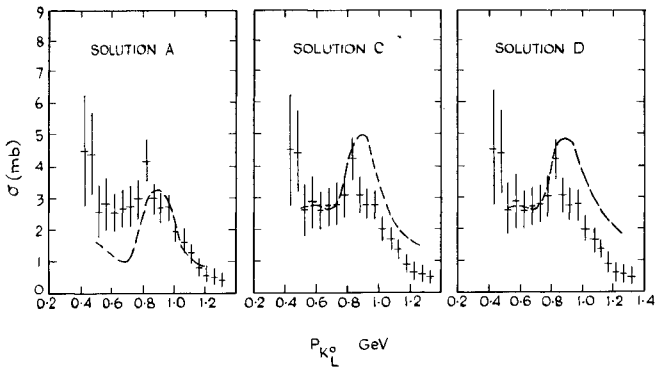

Fig. 9 Preliminary cross sections for $K_L^o p \to K_S^o p$ from the Tel Aviv-Heidelberg collaboration compared with the preduction of the analysis of London (135).

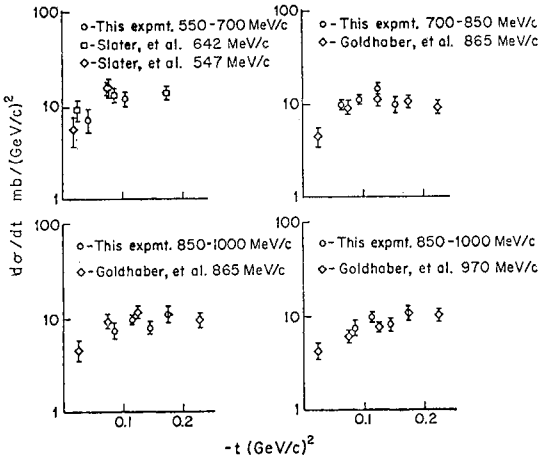

Fig. 10 Comparison of the differential cross section from the reaction $K_L^o p \to K^+ n$ (711) with those of the line reversed reaction $K^+ n(p_s) \to K^o p(p_s)$ from Ref.11

KN and $\bar{K}N$ should be attempted. Preliminary cross section results from the Heidelberg-Tel Aviv experiment[9] are shown in Figure 9, together with the predictions of the London analysis.

Another application of K_L^o interactions presented is in the reaction

$$K_L^o p \rightarrow K^+ n$$

which has been studied by Edelstein et al. (711) between 550 and 1000 MeV/c. This is the time reversed reaction to the deuterium reaction

$$K^+ n \rightarrow K^o p$$

but it is free from the deuterium problems of the latter. The results are identical to those of Goldhaber et al[11] from the deuterium reaction (Figure 10) proving yet again that deuterium experiments are not as hard as they are sometimes made out to be.

2) STRANGENESS 0 (πN) REACTIONS

a) Quasi-two body reactions

The saga of the Berkeley-SLAC (BS) isobar model analysis of $\pi N \rightarrow \pi\pi N$ seems to be nearing its end. For our new readers the story so far: In 1972 a solution (A) was produced which dismayed the theorists as the signs of the $\Delta\pi$ resonant amplitudes were completely at variance with the predictions of $SU(6)_W$. The analysis has always been bedevilled by the famous "energy gap" between 1540 and 1640 MeV where there was no data available to the BS groups. With a little prodding from the theoreticians a second solution (B) was found which has the property that the dominant amplitudes are rotated through 180^o above the gap while retaining approximately the same energy dependence. This solution now gives $\Delta\pi$ signs that agree completely with $SU(6)_W$.

Meanwhile data from the Imperial College-Westfield groups on the reaction $\pi^+ p \rightarrow \pi^+ p \pi^o$ at 1610 MeV has become available and has been analysed by the Berkeley SLAC groups (466). The results are shown in Figure 11 where the solution for the partial waves $\Delta\pi$ SD31, $\rho_{\frac{1}{2}}$ N SS31, $\Delta\pi$ DS33, $\rho_{3/2}$ N DS33 obtained from the IC-Westfield data is given together with solutions A and B for these amplitudes over the whole energy range. The notation for the amplitudes is; reaction, including the total ρ plus nucleon spin for the ρ reactions; incoming L; outgoing L; 2I; 2J. The numbered circles are the IC-Westfield solutions. As the solution has an arbitrary overall phase it is rotated in each case so that the largest amplitude ($\Delta\pi$ SD31) lies as close as possible to the prediction from the K-matrix fit to the BS amplitudes (solid line). It can be seen that the IC-Westfield amplitudes agree very well with solution B but disagree badly with solution A. A numerical comparison is given by the χ^2_{IC} shown on the figure. It is also interesting that internally to the BS analysis the K-matrix fit gives a lower χ^2 for solution B than solution A. There now seems no doubt that B is preferred and A may be discarded, much to the relief of all baryon modelists.

Two new analyses of the $\pi\pi N$ final state have been presented at the conference, one from Baker et al. (383), the Imperial College - Cambridge - Westfield College collaboration (ICW), analysing just the $\pi^+ p$ states and the other from Dolbeau et al., the Saclay group, using both $\pi^+ p$. Figure 1 of Neveu's contribution to the parallel sessions gives the energy points at which the new analyses have been performed. Both analyses have data in the important "gap" region. In view of the importance of these reactions to classification schemes I will make a detailed comparison of them below.

1) Because of the complication of the formalism and the multiplicity of phase conventions involved in these analyses it is encouraging and important that entirely independent programs have been used for the analyses

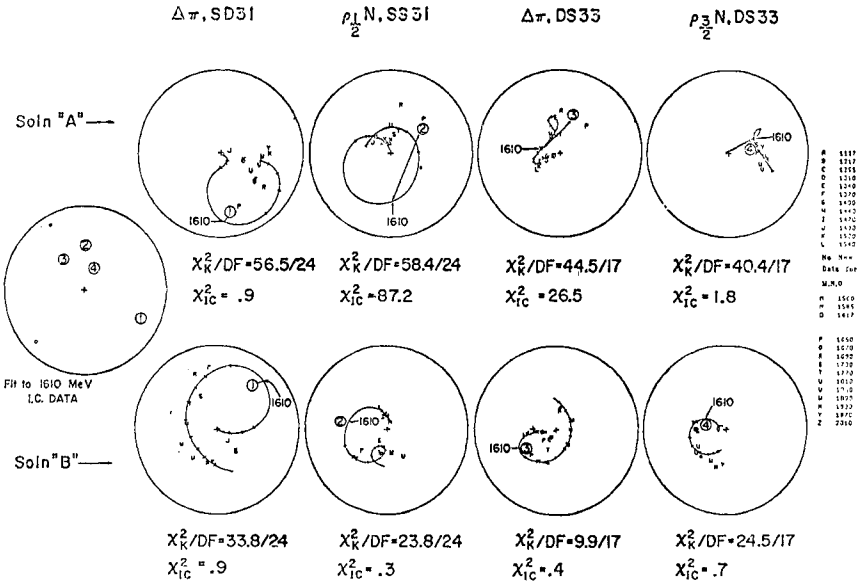

Fig. 11 Comparison of 4 amplitudes from a fit to the Imperial College-Westfield events at 1610 MeV (numbered points in the left circle) with the SB solution A (top row) and solution B (bottom row). The letters are single energy fits, the curves K-matrix fits to the single energy fits.

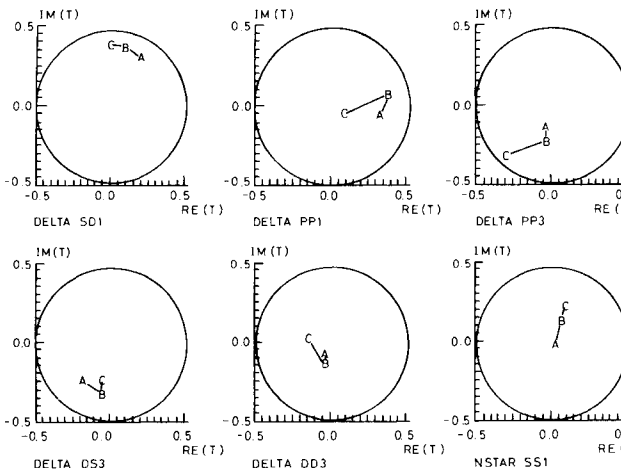

Fig. 12a D15, F15, P33 and D33 amplitudes from the Saclay analysis compared with those of the SB analysis. The numbers correspond to the energy points given in Table I of Neveu's contribution to the parallel sessions. The arrows denote the resonance signs where they can be distinguished.

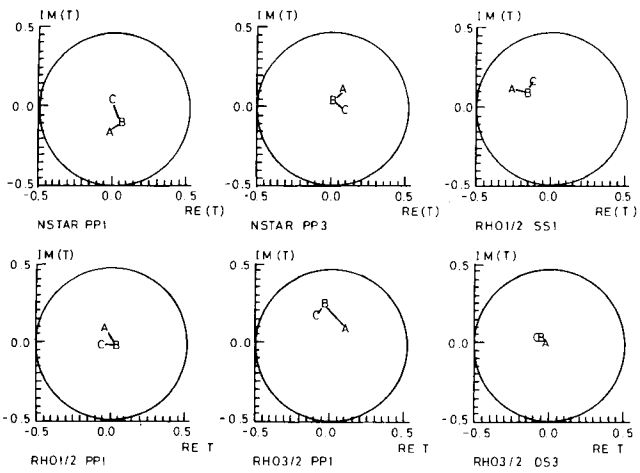

Fig. 12b Argand diagrams from the ICW analysis. A, B and C represent the three energies used in the analysis.

and that they have been thoroughly checked against the BS program.

2) ICW fit the channel $\pi^+\pi^+n$ which was not included in the BS or Saclay analyses principally because it shows evidence for $N_{\frac{1}{2}}^*$ isobars which were not included in their analyses. Because of this ICW include an extra isobar, the P11 N(1470)

3) The fitting procedures are different, ICW and BS using maximum likelyhood and Saclay a χ^2 fit to the coefficients of spherical harmonics averaged over regions of the Dalitz plot.

4) Different forms are used for the production angular momentum barrier; BS and ICW use q^ℓ where q is the centre of mass momentum of the isobar and ℓ is the production orbital angular momentum whereas Saclay use

$$\left[\frac{q/q_o}{(1 + q/q_o)^{\frac{1}{2}}}\right]^\ell$$

where q_o is a constant taken equal to 750 MeV/c. The effect of the Saclay parameterisation is to give a ρ shape with smaller contributions at low $\pi\pi$ masses, thus giving larger ρN amplitudes at low energies.

5) The inelasticities of the Saclay and BS amplitudes were constrained to be less than the inelasticities found from the elastic p.w.a. This was not done in the ICW analysis and inconsistencies are found in the P31 amplitude as discussed below.

6) Both ICW and Saclay introduce more amplitudes than BS, ICW 20 for only the I=3/2 amplitudes and Saclay up to 43 depending on energy compared with 28 for BS.

Some of the Saclay amplitudes are shown in Figure 12a compared with the BS amplitudes. The large amplitudes agree reasonably well but the Saclay analysis contains more small ρN amplitudes probably due to the different barrier factor. Where resonance signs can be determined they agree between the two analyses. The signs are given in Table II of Neveu's report.

The results of the ICW analysis are shown in the Argand diagrams of Figure 12b. The lower two energies are inside the gap and thus cannot be directly compared with BS however at 1670 MeV the amplitudes common to the two analyses agree quite well. The lower energies agree with the K-matrix continuation through the gap except for the PP31 amplitude which is very large. In fact at these energies the inelastic cross section in this amplitude is much larger than that which can be deduced from the elastic channel analyses, though it agrees at 1670 MeV, as shown in Figure 13. It is clearly a problem to be resolved whether or not there is narrow structure in this amplitude. Of the amplitudes not included in the SB analysis the N^* SS31, N^* PP31 and $\rho_{3/2}$ PP31 are all appreciable though it is encouraging that inclusion of these extra amplitudes has not significantly changed the others.

Figure 14 shows the Argand diagrams of solution B. The BS group has used three methods to extract resonance parameters from these amplitudes.

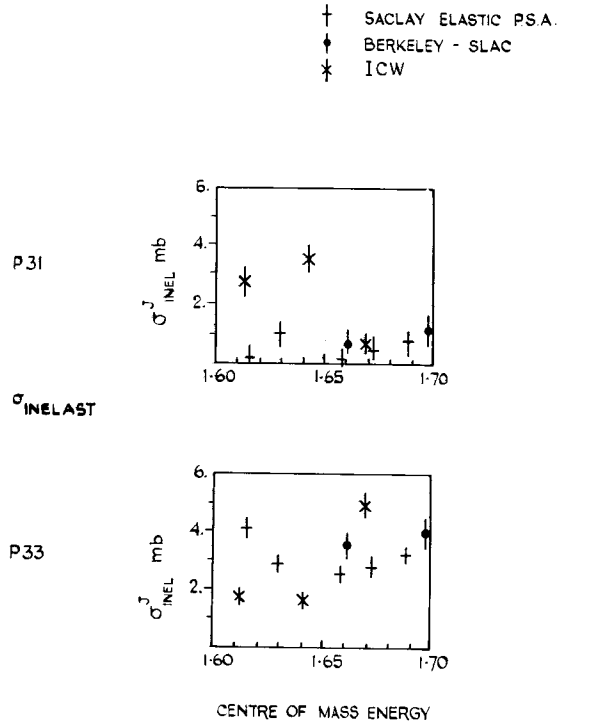

Fig. 13 Inelastic cross section for the P31 and P33 amplitudes from the ICW and SB analyses compared with that predicted by the elastic partial wave analysis of Ayed and Barayre[3].

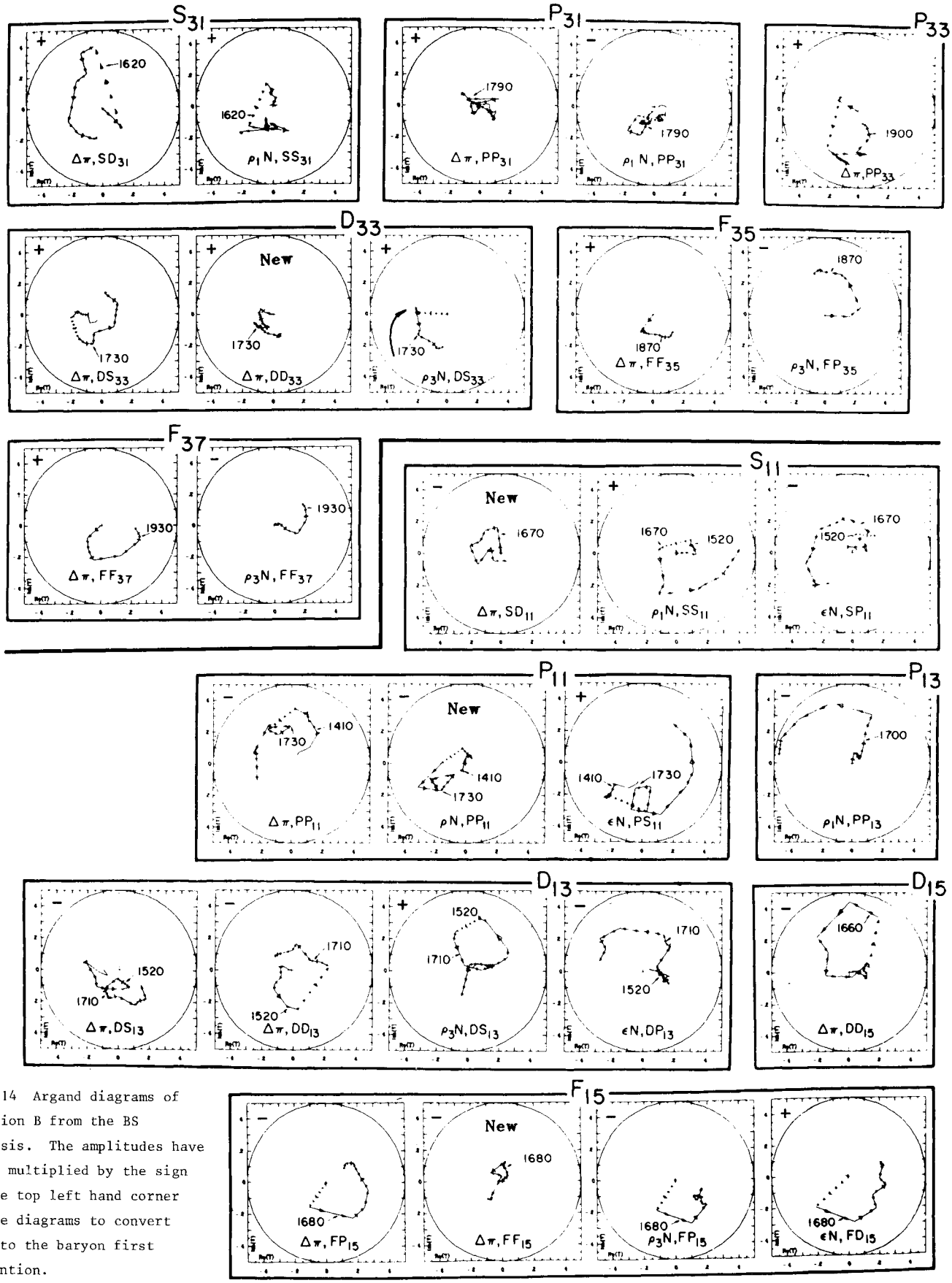

Fig. 14 Argand diagrams of solution B from the BS analysis. The amplitudes have to be multiplied by the sign in the top left hand corner of the diagrams to convert them to the baryon first convention.

(1) Eyeball fits to the Argand diagrams measuring the diameters of resonance circles using ruler and compass and taking masses and widths from the elastic channel analysis of Ayed and Bareyre[3]. (2) Similar eyeball fits to the smoothed unitarised amplitudes of the T matrix calculated from a K matrix fit to the amplitudes, including the elastic amplitudes. (3) Resonance masses and widths were estimated by determining the poles and residues in the T-matrix.

The values obtained from these three methods are given in Table I. The authors recommend method (3) as it has been shown by analysis of the P33 $\Delta(1230)$[12] and their experience with this analysis that the pole values are insensitive to the forms used for the background contributions. This is probably true and probably represents the best method of obtaining consistent sets of numbers from different analyses. However, it is not clear what relationship there is between these numbers and the numbers that should be used, for example, in the comparison of predicted resonance spectra and decay widths with experiment. Some theoretical work on this problem would be useful.

Examination of the results of the three methods in Table I shows that when the resonance circle is large ($\sqrt{xx'} > 0.2$) the agreement is good but for small $\sqrt{xx'}$ (< 0.15) large discrepancies may be found in the magnitudes and even the signs are difficult to determine. The moral is that decisive tests of theory are only possible for the larger amplitudes and it is not surprising if some of the smaller amplitudes disagree. Before abandoning any theory the Argand diagrams should be examined to see how definitive the experimental measurement can be.

The magnitude and particularly the signs of the resonant amplitudes are of the greatest importance in classifying the resonances into their SU(6) multiplets and in testing the various resonance models. This will be dealt with in much greater detail in the review of Rosner but I would like to make a few comments here.

1) The $\Delta\pi$ sign of the P11 N(1420) unambiguously classifies it in a {56, 0+}.

2) The P11 N(1780) is claimed to have the same sign in $\Delta\pi$ as the N(1470) which would again allocate it to a {56, 0+}. However the loop corresponding to the N(1780) sits on a large background and allowance must be made for the difficulty of the extraction of the resonant part of the amplitude.

3) The negative sign of the $\Delta\pi$ PP33 assigns it also to the {56, 0+} as a partner to the Roper resonance.

4) The theoretical interpretation of the ρN signs is more complicated than the $\Delta\pi$ signs but it has been noted by Faiman (190) that they give serious trouble to ℓ-broken SU(6) and the quark model. However before inventing any new models the following experimental points should be considered:
a) As an indication of the difficulty of determining even the sign of the resonance amplitudes, the sign estimation of Faiman disagrees with that of the BS group for several of the smaller amplitudes. Also the transformation to the baryon first sign convention is still in a state of flux, a number of the ρN and εN signs having been changed during the conference. The signs given in Table I are now believed to be current but we probably have to wait for the definitive BS publication where they explain their sign convention before being sure of the signs. The effect of the immediate sign problem is to change the relative signs of the $\rho_{1/2}$ and $\rho_{3/2}$ amplitudes.
b) Faiman has pointed out that in his model the absence of some of the ρ amplitudes that have been

T-matrix property used in estimate	Resonance J^P	Mass (MeV)	Γ (MeV)	$N\pi$ x_1	$N\pi$ Γ_1 (MeV)	$\Delta\pi$ $\sqrt{x_1 x_\Delta}$	$\Delta\pi$ Γ_Δ (MeV)	$\Delta\pi$ $\sqrt{x_1 x_\Delta}$	$\Delta\pi$ Γ'_Δ (MeV)	$N\rho$ $\sqrt{x_1 x_\rho}$	$N\rho$ Γ_ρ (MeV)	$N\epsilon$ $\sqrt{x_1 x_\epsilon}$	$N\epsilon$ Γ_ϵ (MeV)	Check Σx_i
				S_{11}		SD_{11}				$N\rho_1, SS_{11}$		SP_{11}		
I. Argand(T_{1j})	S'_{11}	1520	75	0.34	26	0.00	0			+0.12	3	−0.1	2	0.41 +Nη
II. Tij(K)		1510	100	0.20	20	−0.06	2			+0.09	4	−0.09	4	0.30 +Nη
III. Pole		1496	103		|138| −43°	+*	|11| 0°			+*	|5| 68°	−*	|4| 34°	0.47+Nη
I. Argand(T_{1j})	S''_{11}	1675	150	0.54	81	−0.16	7			+0.23	15	−0.23	15	0.79 +Nη
II. Tij(K)		1660	130	0.45	58	−0.15	6			+0.16	8	−0.25	18	0.69 +Nη
III. Pole		1648	117		|61| −58°	−*	|3| 27°			+*	|5| 12°	−*	|16| −11°	0.72+Nη
				P_{11}		PP_{11}				$N\rho_1, PP_{11}$		PS_{11}		
I. Argand(T_{1j})	P'_{11}	1415	180	0.54	97	−0.30	30			0.00	0	±0.18	11	0.77
II. Tij(K)		1390	200	0.54	110	−0.37	50			−0.23	20	+0.23	20	1.00
III. Pole		1381	209		|136| −68°	−*	|14| −32°			−*	|15| +37°	+*	|10| +108°	0.85
I. Argand(T_{1j})	P''_{11}	1730	165	0.16	28	±0.13	16			+0.32	99	+0.18	31	1.05
II. Tij(K)		1710	75	0.20	15	−0.20	15			+0.20	15	+0.28	30	1.00
III. Pole		1708	17		|3| −146°	−*	|5| −37°			+*	|3| +18°	+*	|7| +130°	1.05
				P_{13}						$N\rho_1, PP_{13}$				
I. Argand(T_{1j})	P_{13}	1695	115	0.14	16					−0.35	101			1.02
II. Tij(K)		1720	150	0.20	30					−0.40	120			1.00
III. Pole		1716	124		|16| −83°					−*	|68| −46°			0.68
				D_{13}		DS_{13}		DD_{13}		$N\rho_3, DS_{13}$		DP_{13}		
I. Argand(T_{1j})	D'_{13}	1524	120	0.56	67	+0.27	16	+0.24	12	+0.32	22	0.0	0	0.98
II. Tij(K)		1520	150	0.60	90	+0.24	15	+0.30	23	+0.24	15	+0.17	7	1.00
III. Pole		1514	146		|88| +2°	+*	|17| +54°	+*	|23| −22°	+*	|22| −90°	+*	|2| 0°	1.03
I. Argand(T_{1j})	D''_{13}	1710	100	0.09	9	+0.15	25	−0.10	11	0	0	−0.2	44	0.89
II. Tij(K)		1710	300	0.1	30	+0.16	75	−0.14	60	−0.07	15	−0.2	120	1.00
III. Pole		1710	607		|14| −138°	+*	|177| −49°	−*	|154| −67°	−*	|6| +162°	−*	|3571| +72°	0.84
				D_{15}		DD_{15}								
I. Argand(T_{1j})	D_{15}	1660	145	0.41	59	−0.45	72							0.90
II. Tij(K)		1660	150	0.45	67	−0.50	83							1.00
III. Pole		1663	146		|162| −17°	−*	|193| +5°							1.06
				F_{15}		FP_{15}		FF_{15}		$N\rho_3, FP_{15}$		FD_{15}		
I. Argand(T_{1j})	F_{15}	1680	125	0.59	74	+0.26	14	0	0	+0.27	15	−0.28	16	0.95
II. Tij(K)		1670	130	0.59	78	+0.25	13	−0.08	1	+0.30	19	−0.30	19	1.00
III. Pole		1668	132		|175| −15°	+*	|15| 0°	+*	|1| −90°	+*	|13| −39°	−*	|28| −32°	1.00
				S_{31}		SD_{31}				$N\rho_1, SS_{31}$				
I. Argand(T_{1j})	S_{31}	1625	160	0.32	51	+0.40	80			−0.18	16			0.92
II. Tij(K)		1600	150	0.40	60	+0.40	60			−0.28	30			1.00
III. Pole		1583	143		|37| −136°	+*	|177| −22°			−*	|26| −152°			0.98
				P_{33}		PP_{33}								
I. Argand(T_{1j})	P''_{33}	1900	205	0.19	39	−0.36	140							0.87
II. Tij(K)		1640	300	0.10	30	−0.30	270							1.00
III. Pole		1609	323		|177| −77°	−*	|157| −94°							0.72
				D_{33}		DS_{33}		DD_{33}		$N\rho_3, DS_{33}$				
I. Argand(T_{1j})	D_{33}	1725	190	0.17	32	−0.25	70	0	0	+0.20	45			0.77
II. Tij(K)		1680	240	0.20	48	−0.24	72	−0.10	12	+0.30	108			1.00
III. Pole		1681	245		|136| +16°	−*	|113| +29°	+*	|28| −145°	+*	|84| +104°			1.06
				F_{35}				FF_{35}		$N\rho_3, FP_{35}$				
I. Argand(T_{1j})	F_{35}	1870	255	0.14	36			−0.12	26	−0.28	143			0.80
II. Tij(K)		1830	220	0.18	40			−0.20	48	−0.33	132			1.00
III. Pole		1813	193		|132| −46°			−*	|140| +19°	−*	|96| −59°			0.87
				F_{37}		FF_{37}				$N\rho_3, FF_{37}$				
I. Argand(T_{1j})	F_{37}	1930	235	0.41	96	−0.25	36			−0.18	19			0.64+?
II. Tij(K)		1925	240	0.40	96	−0.32	60			−0.24	36			0.80+?
III. Pole		1924	258		|185| −17°	−*	|177| −9°			−*	|139| +52°			1.00+?

*In Method III we get the widths directly from the T-matrix residues, and are unconcerned with $\sqrt{x_1 x_\Gamma}$, except for its sign.

Table I Magnitude and signs of the resonance couplings from the BS analysis obtained by the three methods described in the text.

omitted from the analysis by BS is puzzling. Clearly another model would give different predictions and Faiman himself has produced one (191) but when the $\rho_{1/2}$ amplitude is as strong as in the PP13 case it is strange that there is no $\rho_{3/2}$ amplitude at all. It will also be remembered that several ρ amplitudes are appreciable in the ICW and Saclay analyses but have been omitted from the BS.

(c) Some of the problems in this channel can be understood by looking at the respective angular distributions for ρN and $\Delta\pi$ shown in Figure 15 from the experiment of Kernan et al[13], data included in the BS analysis. It can be seen that whereas the $\Delta\pi$ angular distributions are approximately symmetric and change rapidly with energy the ρN distributions are strongly forward peaked and relatively unchanging. Thus whereas the $\Delta\pi$ amplitudes are relatively clean with little background and clear resonance loops, the ρN amplitudes have very strong backgrounds, as in the elastic channel, and the resonance structure is hard to disentangle particularly in the low partial waves.

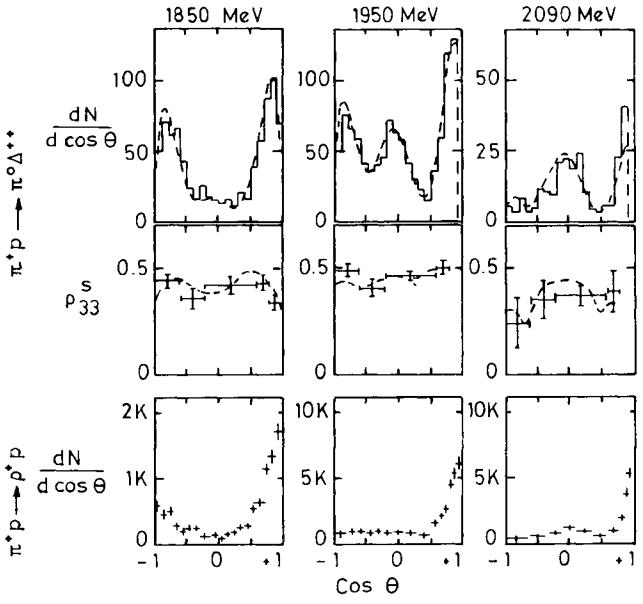

Fig. 15 Angular distributions for $\pi^+p \to \Delta^{++}\pi^0$ and $\pi^+p \to p\rho^+$ at three centre of mass energies taken from Kernan et al.[13]

Also concerning the decay of resonances into vector mesons, two papers are submitted reporting a $p\omega$ enhancement at approximately 1800 MeV. One is from the Nijmegen-Amsterdam collaboration (434) giving data on the reaction $K^-p \to K^-p\pi^+\pi^-\pi^0$ at 4.2 GeV/c and the second from Linglin et al. (978) on the reaction $\pi^+p \to \pi^+p\pi^+\pi^-\pi^0$ at 13.7 GeV/c taken in the SLAC 40" triggered bubble chamber. The $p\omega$ mass plots are shown in Figure 16. The masses and widths (approximately 120 MeV) are in good agreement. The effect has also been reported in π^-p at 7 GeV/c[14] and K^+p at 12 GeV/c[15]. The major problem is whether the effect is truely resonant or a low mass Deck-type enhancement in $p\omega$. The narrow width and its appearance in such varied reactions over a wide range of incident energies makes me favour the resonance interpretation. The spin-parity is, of course, undetermined from the production experiments but the SLAC-Berkeley analysis finds a P13 resonance with a very strong $p\rho$ decay at a slightly lower

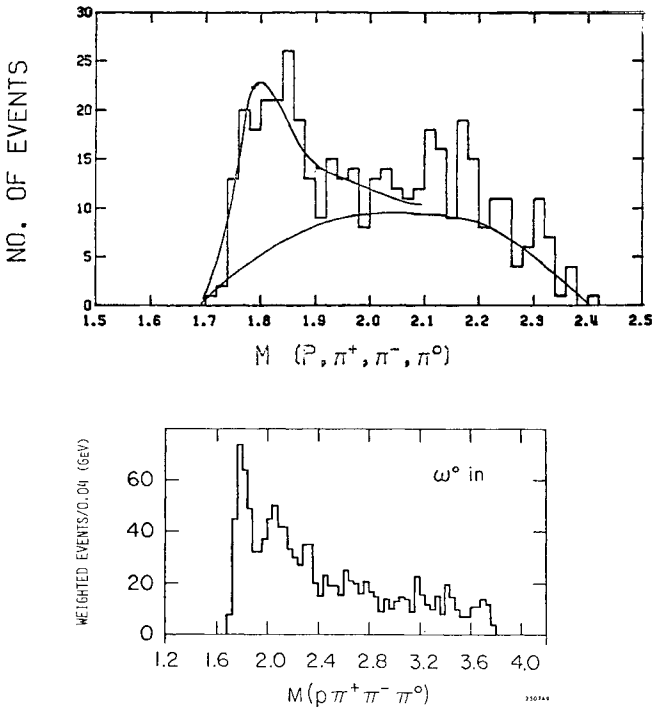

Fig. 16 ωp effective mass plots from (a) $K^-p \to K^-p\omega$ at 4.2 GeV/c (434) and (b) $\pi^+p \to \pi^+p\omega$ at 13.7 GeV/c (978).

mass and an analysis of the channel $K^-p \to \Lambda\omega$[16] found evidence for a $\Lambda\omega$ resonance close to threshold whose spin parity could not be determined but which was consistent with P3. There may thus be an indication of the presence in this mass region of an SU(3) octet with a strong coupling to the vector mesons.

No analysis of the πN elastic channel is presented and it seems that at least below 2.0 GeV/c these analyses have been pushed almost as far as it is worthwhile to take them. The remaining doubtful structures are so small that both a large increase in the statistics of the experiments and a very detailed knowledge of the systematics of the analysis methods would be required to sort them out. Instead it would seem more profitable to study the inelastic two body channels ηN, ΛK, ΣK which have been strangely neglected. As well as the possibility of a weak resonance in πN showing up more strongly in these channels the signs of the resonant amplitudes give valuable information for the classification of the resonances in the same way as the $\Lambda\pi$ and $\Sigma\pi$ channels in $\bar{K}N$.

However a worthwhile effort is being made by Hodgkinson et al. (132) to compile and combine all available πN data. In a very complicated fitting procedure they attempt to remove normalisation, calibration and resolution errors, finally producing a consistent set of data. Anybody who has data which could be added to the compilation or who is thinking of embarking on a similar compilation is urged to contact these authors.

New data on the total cross sections for the reactions

$$\pi^- p \to \Lambda K^0$$
$$\to \Sigma^- K^+$$
$$\to \Sigma^0 K^0$$

at centre of mass energies between 1630 and 1780 MeV are presented by Baton et al. (402). This is part of a high statistics bubble chamber study of associated production between ΛK threshold and 2000 MeV. Figure 17 shows the cross section for the Σ channels together with the rest of the world's data (notable mostly for its sparseness) and the prediction of the partial wave analysis of Langbein and Wagner[17]. It is clear that the rise of the total cross section from threshold is much steeper than that found by the partial wave analysis indicating possible extra resonance behaviour. Final results from this experiment together with the counter experiments presently studying the ΛK and ηN channels are eagerly anticipated.

Using the Barrelet zeros method Baker (1006) has reanalysed the ΛK data previously analysed by Lovelace and Wagner. He finds that the original Lovelace and Wagner solutions suffered from discontinuities in the zero trajectories in the same manner as the similar analysis of Langbein and Wagner of the $\bar{K}N$ channels[18]. This seems to be an occupational hazard of shortest path methods performed on inadequate data. By requiring continuous smooth zero trajectories and a minimal set of partial waves he finds four ambiguous solutions.

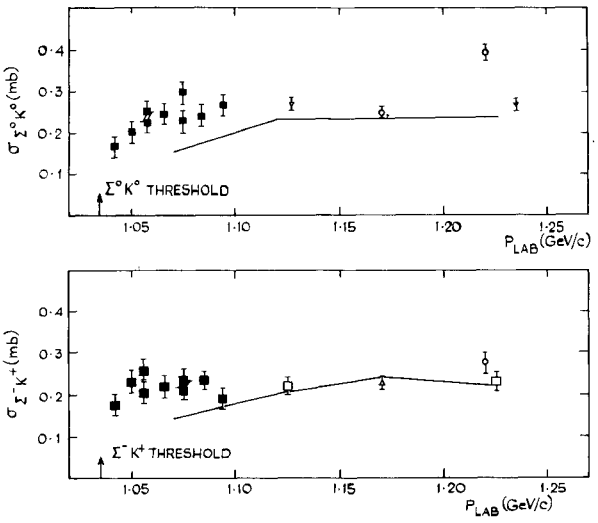

Fig. 17 Cross section for $\pi^- p \to \Sigma^0 K^0$ and $\pi^- p \to \Sigma^- K^+$ from Baton et al. (402), solid squares, together with data from other experiments. The line is the prediction of the partial wave analysis of Langbein and Wagner[17].

TABLE II

	From ΛK Analysis				From elastic channel	
Amplitude	Mass	Width	Branching Fraction	Phase	Mass	Width
S11	1725	90	0.09	0^{o}	1672	179
P11	1705	70	0.20	100^{o}	1729	217
P13	1670	30	0.01	25^{o}	1696	117
D13	1725	70	0.09	-60^{0}	1710	100

Two of them were discarded as having an unphysical S11 amplitude and the other two are practically identical. Fixing the arbitrary overall phase at each energy by requiring the P11 amplitude to have a Breit-Wigner phase variation yields the Argand diagrams shown in Figure 18. Resonances can be seen in the S11, P11, P13 and D13 amplitudes and their parameters are given in Table II together with the parameters of Ayed and Bareyre[3] from their analysis of the elastic channel. The masses agree quite well but the widths are systematically smaller than those found in the elastic channel.

In the channel $\pi+p \to \Sigma^{+}K^{+}$ there is an amusing possibility to search for exotic baryons [38]. The only non exotic states allowed are members of {10}'s which must all have the same sign for their amplitudes at resonance. Any resonance with the opposite sign has to be a member of a {27}, making such states very easy to detect in this channel.

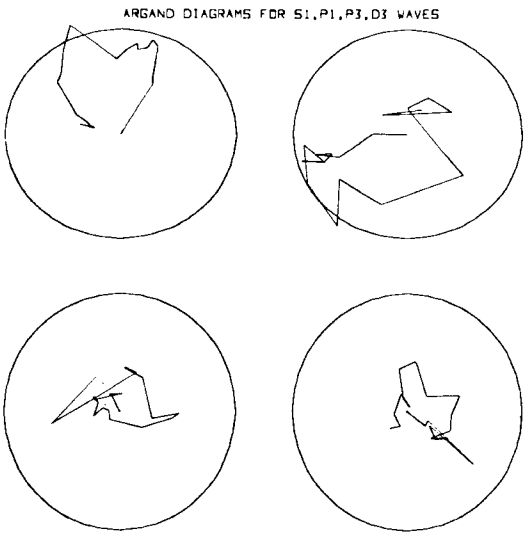

Fig. 18 Argand diagrams of Baker (1006) for the reaction $\pi^{-}p \to \Lambda K^{o}$. The circles shown have a diameter of 0.32 and should not be confused with the unitary circle.

Finally to end this section on a high note, at least in mass, an experiment by Baker et al (687) has measured the backward π+p elastic cross section from 2 to 6 GeV/c obtaining the results shown in Figure 19. Rey et al. (689) have fitted this cross section with a sum of resonances plus dualised Regge background and obtained the following parameters for the high mass Δ resonances.

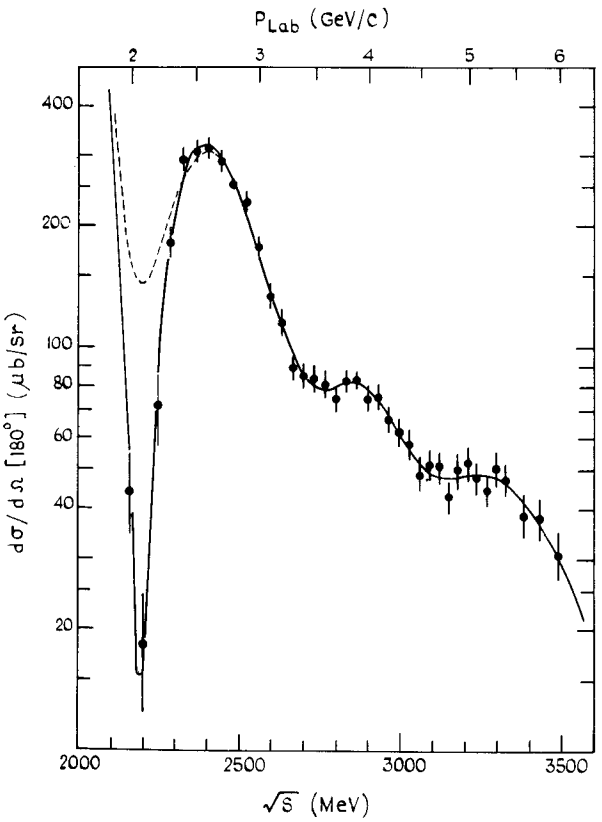

Fig. 19 The 180^{o} differential cross section for $\pi^{+}p$ elastic scattering as a function of centre of mass energy. The solid line is a fit including the resonances shown in Table III plus lower mass resonances and a Regge background. The dashed curve is the best fit without the Δ(2200).

TABLE III

	J^P	Mass (Mev/c^2)	Width (MeV/c^2)	X (J + 1/2)
Δ (2200)	$?^-$	$2196\ ^{+31}_{-26}\ \pm15$†	$302 \pm 120 \pm 23$	$.81\ ^{+.36}_{-.21} \pm .18$
Δ (2420)	$?^+$	$2404 \pm 48 \pm 15$	$484 \pm 75 \pm 4$	$.94\ ^{+.37}_{-.16} \pm .05$
Δ (2850)	$?^+$	$2883\ ^{+21}_{-23} \pm 5$	$380\ ^{+120}_{-180} \pm 21$	$.28\ ^{+.12}_{-.18} \pm .01$
Δ (3230)	$?^+$	$3296\ ^{+56}_{-55} \pm 23$	$687\ ^{+1000}_{-280} \pm 43$	$.45\ ^{+.04}_{-.08} \pm .05$

Results of fitting in energy region 2 to 6 GeV/c

†The errors on our parameters are given in two parts. The first is the statistical error, which was obtained as described in the text. In general, these errors are correlated. The second is the systematic error.

The fact that there are observable resonances at masses of 3200 MeV and incident beam momenta of 6 GeV/c is perhaps worrying to the Regge phenomenologist and intimidating to the partial wave analysist. As I shall discuss later, the pattern of the high spin resonances, which are presumably those being seen here, is extremely characteristic of the SU(6) multiplets present; high spin Δ's corresponding to {56}'s and high spin N*'s to {70}'s. Thus partial wave analyses at these high momenta which did nothing but determine the resonances in the highest partial waves would be valuable clues to the high lying supermultiplet structure. The aspiring partial wave analyst in the 3-4 GeV/c region should thus not be put off by his inability to determine the s waves but should plough on regardless and extract what he can, he could still make very valuable contributions to classification schemes.

3) STRANGENESS -1 ($\bar{K}N$) REACTIONS

Results from the second generation $\bar{K}N$ bubble chamber formation experiments taking between 1.0 and 1.5 events/μb/momentum point are now becoming widely available. Papers are presented from the CERN-Heidelberg-Munich collaboration on $\bar{K}N$ (176), from the Rutherford-Imperial College collaboration on $\bar{K}N$, (350), $\Lambda\pi$ (351) and $\Sigma\pi$ (349) and from the Chicago-LBL experiment on $\Sigma^o\eta$ (559).

Compared with the πN system one is still struck by the small contribution made by electronics experiments. Only one paper is presented to the conference, measuring the real part of the forward elastic scattering (669). Counter techniques are surely far enough advanced to handle the $\Lambda\pi^o$ and $\bar{K}^o n$ channels, even if they cannot manage Σ's, and high statistics measurements particularly on polarised targets would clean up the field. With the new intense K^- beams becoming available if even one group could be weaned away from 400 GeV/c a dramatic advance could be made.

Partial wave analyses are presented covering various energies and final states. No multichannel analysis has been attempted though the RHEL-IC groups have made coordinated single channel analyses of the three channels $\bar{K}N$, $\Lambda\pi$, $\Sigma\pi$.

$\bar{K}N$ final states

Baillon et al (669) present measurements of the real parts of the forward scattering amplitudes. They have made a dispersion relation analysis predicting the real parts over the complete energy region. The values agree well with those found by an earlier $\bar{K}N$ partial wave analysis[19] and have been used in the analysis of Hemingway et al (176).

Two energy dependent partial wave analyses have been presented, one by Hemingway et al. (the CERN-Heidelberg-Munich collaboration (CHM)) (176) covering the energy range 1840 to 2230 MeV and incorporating new data on

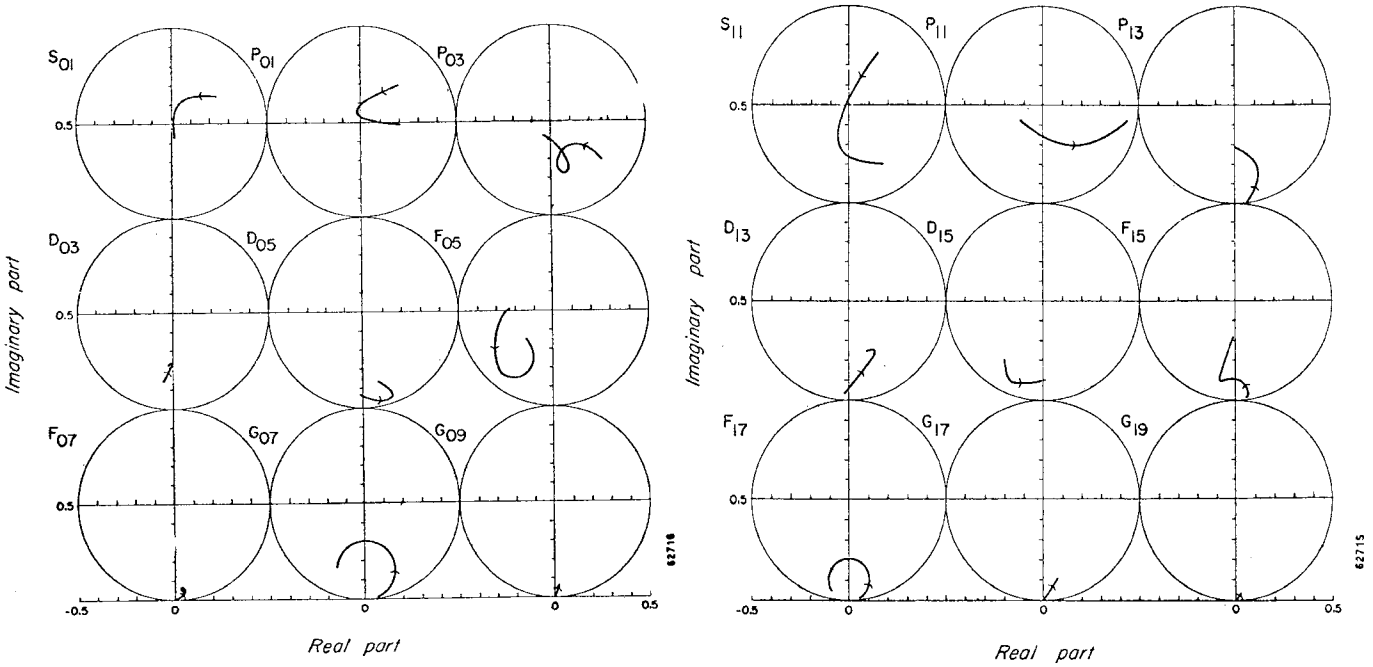

Fig. 20 Argand diagrams for the reaction $K^- p \to \bar{K}N$ from the analysis of Hemingway et al. (176)

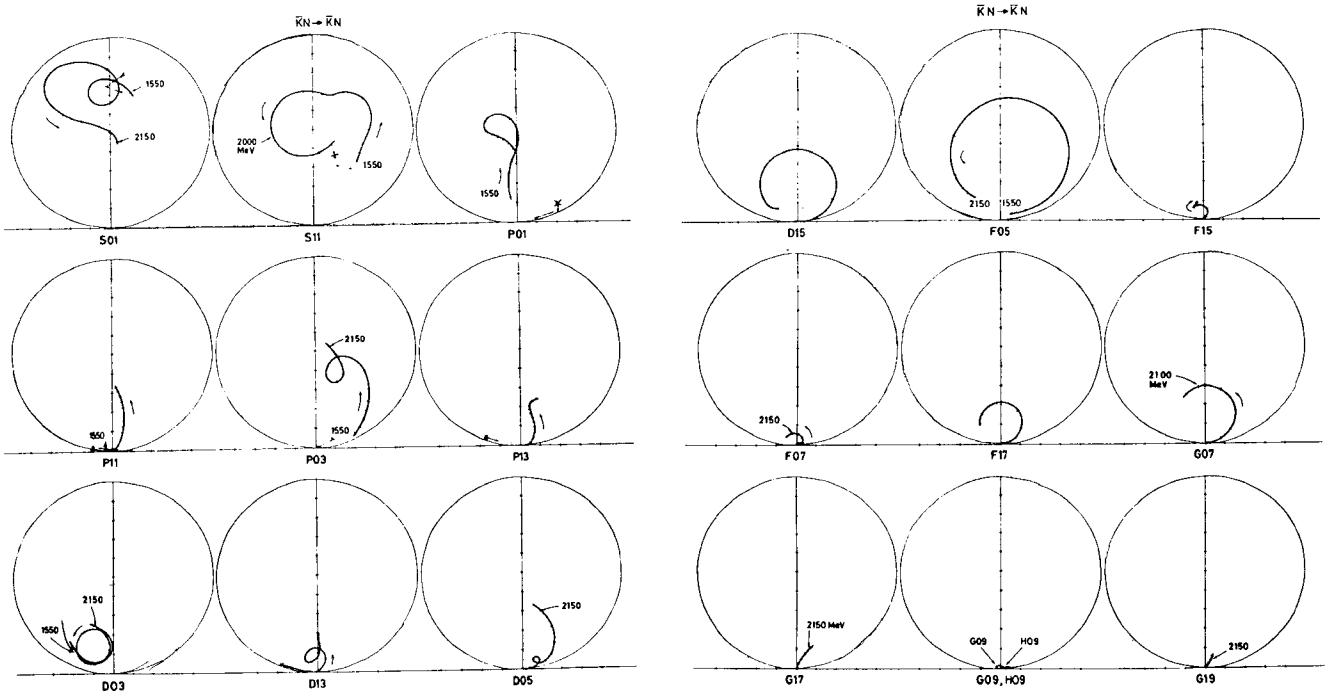

Fig. 21 Argand diagrams for the reaction $K^- p \to \bar{K}N$ from the analysis of Van Horn et al. (350). The dashed curves are the results of the analysis of Tripp [21] in the centre of mass energy region 1490-1540 MeV. The cross marks the highest energy point.

$\bar{K}^0 n$ and $K^- p$ differential cross sections at 23 energy points. The other from Van Horn et al. (350), the RHEL-IC collaboration, covering the range 1540 to 2170 MeV with new data at eleven points between 1770 and 1960 MeV. Both analyses make use of most other available data in their energy regions. The Argand diagrams of the two analyses are shown in Figure 20, Hemingway et al and Figure 21, Van Horn et al. Remembering that Hemingway et al. go to higher energies, comparison shows that the D waves and above are in good agreement and also that they agree well with earlier analyses below 1.2 GeV/c[20] and above 1.2 GeV/c [19]. Figure 22 shows the S and P waves of the two analyses plotted together with the amplitudes from Refs. 19 and 20. The P3 amplitudes agree quite well but the $J=\frac{1}{2}$ amplitudes show rather large differences. This

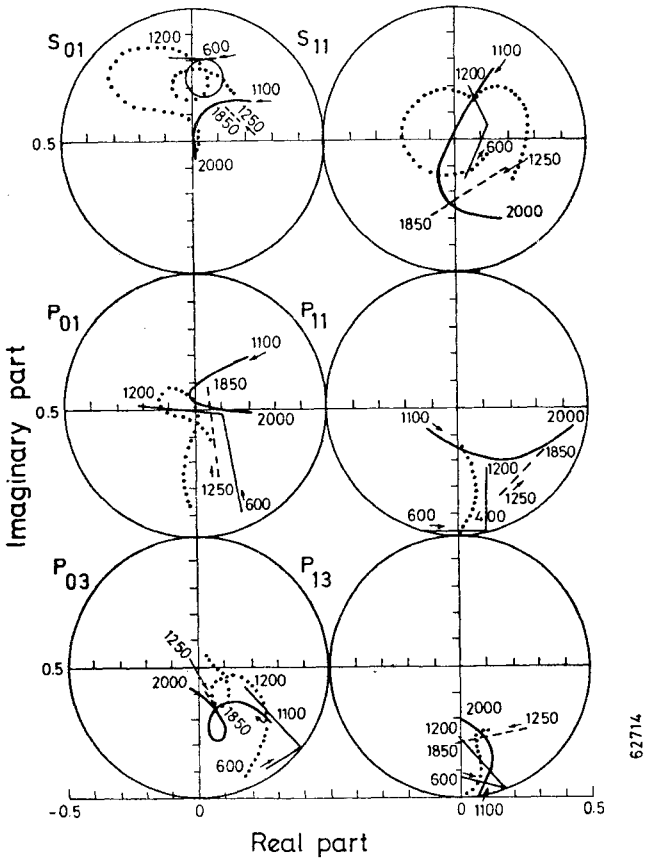

Fig. 22 Comparison of the s and p wave amplitudes of Hemingway et al. (thick line), Van Horn et al. (dotted line), CHS energy dependent analysis[20] (thin line) and the CRSS analysis[19] (dashed line).

was expected by the authors of paper 350 and Ref.19 who concluded that the S and P waves are poorly constrained. In fact the low energy agreement is not too bad, only the analyses starting above 1 GeV/c are in serious disagreement. Since Van Horn et al have the advantage of continuation from low energies their set of amplitudes must be considered the most reliable. However resonance claims above 1800 MeV in the spin $\frac{1}{2}$ amplitudes should be treated with caution. Figure 21 also shows as dashed lines the results of the analysis of Tripp[21] in the very low energy region 1490 to 1540 MeV. The cross marks the highest energy points and this should be nearly coincident with the lowest point of Van Horn et al. The agreement is good for the large S wave amplitudes but some of the smaller amplitudes, e.g. P01 P13 and D13 do not connect very well.

The resonance parameters of Hemingway et al are given in Table IV and of Van Horn et al in Table V. Both analyses see the F07 $\Lambda(2100)$ and P03 $\Lambda(1890)$ which have been suggested in earlier analyses of this channel. Agreement is generally good for the parameters of the dominant resonances but Van Horn et al. find a number of weaker candidates that are not required by the analysis of Hemingway et al. It is interesting that both analyses confirm the findings of Ref. 19 that the width of the G07 $\Lambda(2100)$ is large, of the order of 250 MeV, as distinct from the 60-140 MeV given in the Particle Data Group tables. This channel is the only one in which it is possible at present to measure this width with any accuracy, in the $\Sigma\pi$ channel the amplitude at resonance is much smaller and the data uncertainies much larger and in the total cross section the contribution of the G07 amplitude cannot be separated from the other partial waves.

	Mass (E_R) (MeV)	Width T_{E_R} (MeV)	Elasticity (x)	Phase (ϕ) (Radians)
P_{03}	1890 ± 10	100 ± 10	.25 ± .03	0.78 ± .25
D_{05}	{1825}	{105}	{.08}	{0.}
D_{15}	{1765}	{120}	{.41}	{0.}
F_{05}	{1820}	{84}	{.62}	{0.}
F_{15}	1901 ± 5	99 ± 15	.10 ± .02	-0.40 ± .15
F_{07}	2093 ± 20	147 ± 10	.05 ± .02	-0.09 ± .15
F_{17}	2027 ± 5	174 ± 15	.21 ± .03	{0.}
G_{07}	2104 ± 10	221 ± 25	.31 ± .04	{0.}

TABLE IV Resonance parameters obtained by the analysis of Hemingway et al. (176) for the reaction $K^-p \to \bar{K}N$.

Λπ final state

Three analyses of the Λπ channel are presented, two by myself and one by the RHEL-IC group. The first (522) is an analysis in a very narrow (25 MeV) energy region around the total cross section bump at 1580 MeV reported by K K Li at the Purdue conference[22]. The data, from the CHS collaboration, is split into 10 MeV/c incident momentum bins. The angular distributions are shown in Figure 23 and the Legendre A and B coefficients in Figure 24. The angular distributions can be seen to change from having a forward dip to a strong forward peak in this narrow region. As the energy range is so narrow the background amplitudes in the partial wave analysis can be taken as constants. A fit with constant S and P waves plus the tails of the D13 Σ(1660) and D15 Σ(1765) gave a $\chi^2/_{NDF}$ of 105.5/45 (dashed line in Fig.24). The largest discrepancy is in the A_3 and B_3 coefficients which require the presence of strong D waves. It is found that only the introduction of a D3 resonance produces an acceptable $\chi^2/_{NDF}$ (59.0/42), the full curve in Fig.24. The parameters of the resonance are

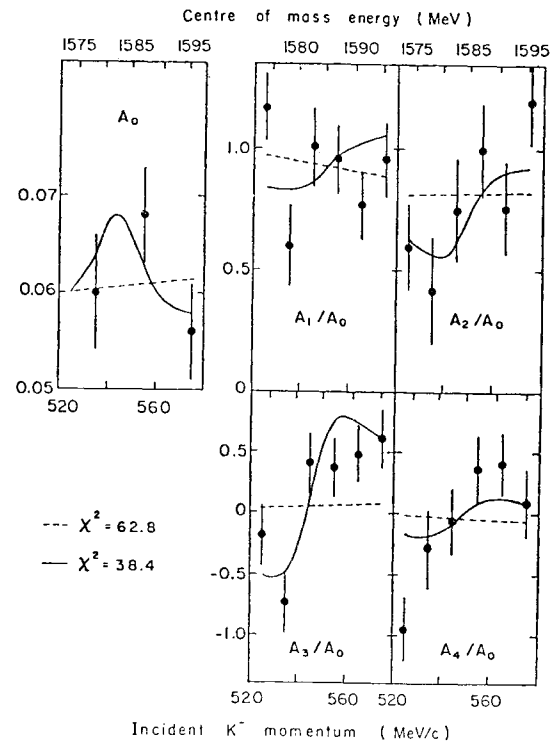

Fig. 23 Angular distributions for $K^-p \to \Lambda\pi^0$ in 10 MeV/c incident momentum bins between 520 and 580 MeV/c.

TABLE V: Y* Resonance Parameters[†]

Channel:		Partial Wave S01	S11	P01	P11	P03	P13	D03	D13	D05	D15	F05	F15	F07	F17	G07
$\bar{K}N$	Mass :	1665	1770	1813	1657	1905		1693	1665	(1822)	1774	1820	1917	2120	2035	2096
	Γ :	35	85	110	200	62	No	34	26	(111)	143	80	100	90	168	274
	t :	.20	.16	.30	.06	.19	consistent states	.21	.09	.06	.41	.60	.03	.07	.22	.29
	Status:	Established	Probable	Prob	Poss	Prob		Est	Est	Est	Est	Est	Est	Prob	Est	Est
	Mass :	1860	1960		2008			1874	1922							
	Γ :	310	189		500			330	192							
	t :	.50	.48		.07			.18	.10							
	Status:	Possible	Prob		(?)			Poss	Poss							
$\Sigma\pi$	Mass :	1679	1987	1605	1697	1915	1843	1682	(1662)	1822	(1774)	(1820)	1925		2040	2136
	Γ :	31	104	260	240	50	250	58	(40)	111	(140)	(80)	110		175	156
	t :	-.22	-.16	-.20	-.13	-.12	.05	-.25	.21	-.16	.08	-.32	-.15		-.10	.14
	Status:	Est	Poss	Prob	Poss	Poss	Poss	Est	Est	Est	Est	Est	Est		Est	Est
	Mass :								2070			2122	2180			
	Γ :								500			164	150			
	t :								-.10			.18	.09			
	Status:								(?)			Prob	Poss			
$\Lambda\pi$	Mass :		1700		1630				1658		1772		1920		2040	
	Γ :		60		270				30		135		100		173	
	t :		-.14		±.10				.08		-.29		-.08		.19	
	Status:		Prob		Poss				Est		Est		Est		Est	
	Mass :		2020						1912				2240			
	Γ :		180						170				300			
	t :		.10						±.08				-.10			
	Status:		Poss						Poss				(?)			

[†] Mass = Energy at Resonance (MeV), Γ = Full Width (MeV), t = Amplitude at Resonance.
Parameters in brackets have been constrained as discussed.

Table V Resonance parameters from the analyses of the RHEL-IC collaboration of the reactions $K^-p \to \bar{K}N$, $\Sigma\pi$, $\Lambda\pi$, (350, 349, 351). The status of each resonance estimated by the same authors is also given.

M = 1582±4 MeV, Γ = 11±4 MeV and amplitude at resonance = +0.10±0.02. Thes parameters are in good agreement with those found for the total cross section bump where the width was less than the experimental resolution (≈ 30 MeV).

Preliminary data from Cho et al.(105) on the reaction $K_L^o p \to \Lambda\pi^+$ in the same momentum region supports the rapid change in the angular distribution though there may be some disagreement in their higher momentum distributions where their statistics is smallest.

The second Λπ analysis is an energy independent analysis from 1540 to 2150 MeV (1011). It uses a new method for energy continuation to ensure smooth solutions. At each energy point an extra χ^2 is added in the fits depending on the distance the solution moves from the solution at the previous energy. An iterative procedure is adopted in that if the solution wishes to move, indicated by a high constraint χ^2, the fit is repeated now constraining the solution to lie close to that found in the first iteration. This is repeated until the constraint χ^2 is small. Thus the solution can move but unless it is absolutely required by the data it will not. Solution paths are selected from the many ambiguous paths by requiring Breit Wigner resonance behaviour for the D15 Σ(1765) and F17 Σ(2030). This plus continuity of the Barrelet zeros is sufficient to produce a unique solution between 1750 and 2060 MeV. Below and above this our lack of knowledge of the dominant amplitudes cause ambiguities, though below 1750 there are only two possible solutions. These are Barrelet ambiguities of each other, involving flipping a complete zero trajectory below 1750 MeV at which point it is a purely real zero. One of these solutions may be preferred as its amplitudes in the Σ(1580) region agree well with those found in paper 522 whereas the second solution has a set of amplitude which

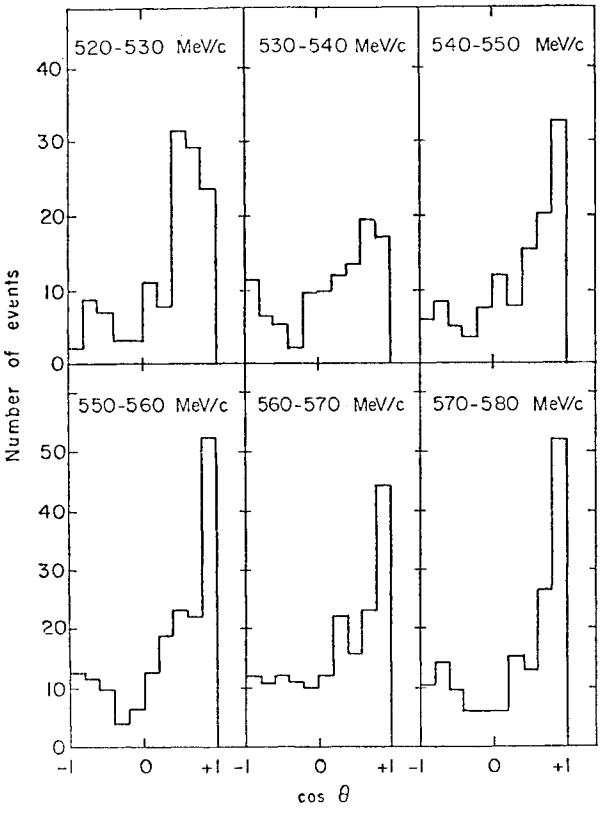

Fig. 24a A_o and A_1/A_o coefficients as a fraction of the incident K^- momentum and centre of mass energy.

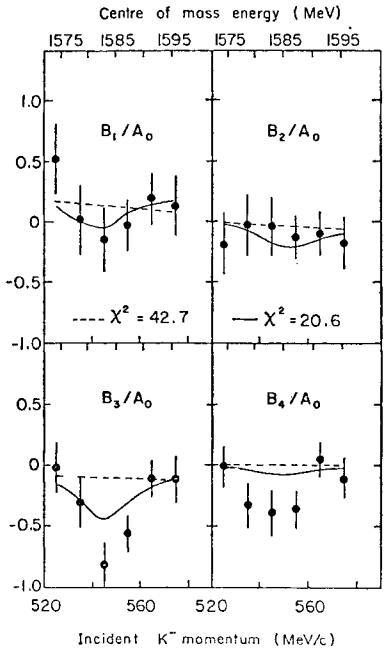

Fig. 24b B_1/A_o coefficients. The solid line is the best fit without a 3/2 $^-$ Σ(1580) resonance, the dashed line with the resonance.

give a high χ^2 in this region. The amplitudes obtained from the energy continuation were fitted with normal background plus resonance terms to obtain resonance parameters. Only backgrounds quadratic in the centre of mass momentum were required over the complete energy range. The resonance parameters are given in Table VI for the two solutions. Solution 1 is the preferred solution. The Argand diagrams obtained from the fits are shown in figure 25 for solution 1 and the S and P waves of solution 2 in figure 26. The D waves and above are identical in both solutions.

The $\Lambda\pi$ analysis of Clayton et al from the RHEL-IC collaboration (351) is a standard energy dependent analysis very similar to the analysis of Van Horn[23] and comes to essentially identical conclusions.

The S and P wave Argand diagrams are shown in figure 27. The D waves and above are similar to those of Litchfield (1011).

Four recent analyses of this channel are available for comparison, Litchfield (1011), Clayton et al (351), Lea, Martin, Moorhouse and Oades[24] (LMMO) and Baillon [25]; the analyses of Van Horn[23] is omitted because of its similarity to Clayton et al and that of Langbein and Wagner[26] because of the demonstrated problems with the lack of continuity of its Barrelet zeros[18]. One finds that, as in

Partial Wave	Mass (MeV)	Width (MeV)	Amplitude ($\sqrt{x}x'$)	ϕ (rads)
D13	1685 ± 20	85 ± 25	+0.06 ± 0.02	0.4 ± 0.3
D13	1950 ± 30	150 ± 75	-0.04 ± 0.02	0.0 ± 0.5
D15	1775 ± 10	125 ± 15	-0.25 ± 0.02	0.0 (fixed)
F15	1920 ± 30	70 ± 20	-0.06 ± 0.02	0.7 ± 0.3
F17	2035 ± 15	180 ± 20	+0.18 ± 0.02	0.0 (fixed)

Solution 1

Partial Wave	Mass (MeV)	Width (MeV)	Amplitude ($\sqrt{x}x'$)	ϕ (rads)
S11	1780 ± 30	140 ± 30	-0.12 ± 0.02	-0.1 ± 0.3
P11	1660 ± 30	80 ± 40	-0.04 ± 0.02	1.1 ± 0.8
P11	1770 ± 20	80 ± 30	-0.08 ± 0.02	-0.5 ± 0.5
P11	1960 ± 30	260 ± 40	-0.12 ± 0.02	0.9 ± 0.4
P13	1720 ± 30	120 ± 30	+0.11 ± 0.02	1.2 ± 0.3
P13	2120 ± 40	240 ± 50	-0.13 ± 0.04	0.5 ± 0.3

Solution 2

Partial Wave	Mass (MeV)	Width (MeV)	Amplitude ($\sqrt{x}x'$)	ϕ (rads)
S11	1700 ± 30	160 ± 50	-0.13 ± 0.03	-0.4 ± 0.4
P13	2140 ± 40	200 ± 50	-0.13 ± 0.04	0.0 ± 0.4

Table VI/Resonance parameters from the analysis of Litchfield of the reaction $\bar{K}p \to \Lambda\pi$ (1011). The d wave and above resonances are the same in both solutions. The resonance parameters in the s and p waves are given separately for the two solutions.

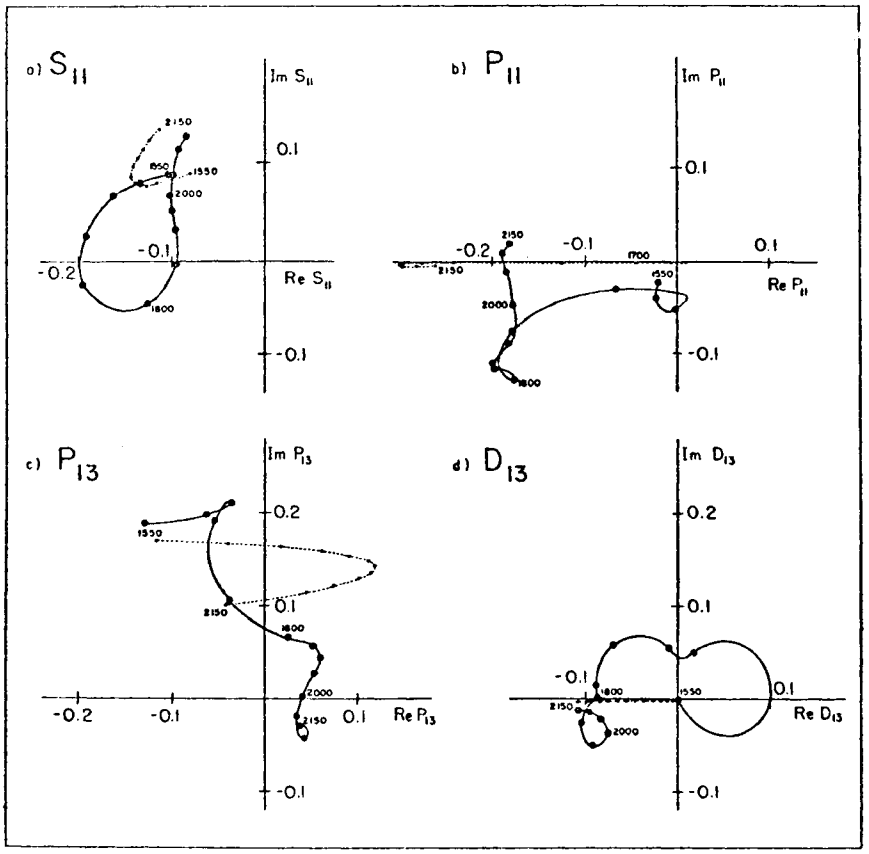

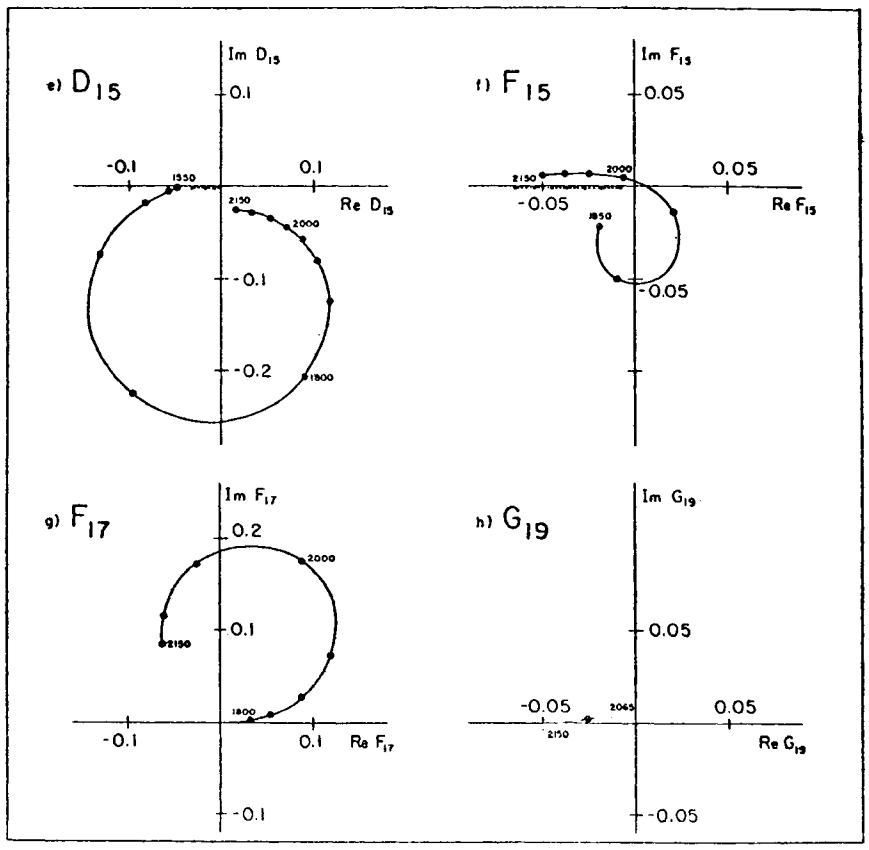

Fig. 25 Argand diagrams for the reaction $\bar{K}p \to \Lambda\pi$ from solution 1 of Litchfield (1011). The solid line is the full amplitude, the dashed line the background contribution.

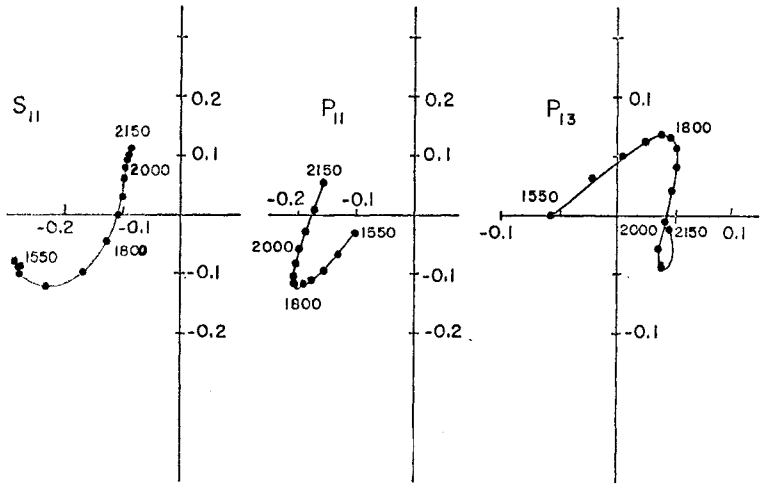

Fig. 26 Argand diagrams of the s and p waves of solution 2 of Litchfield (1011). The d waves and above are identical to solution 1.

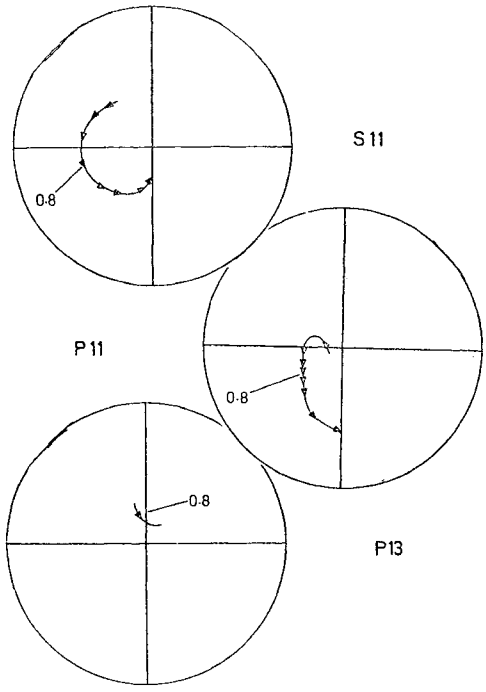

Fig. 28 s and p wave argand diagrams for the reaction $\bar{K}p \to \Lambda\pi$ from the multichannel analysis of LMMO [24].

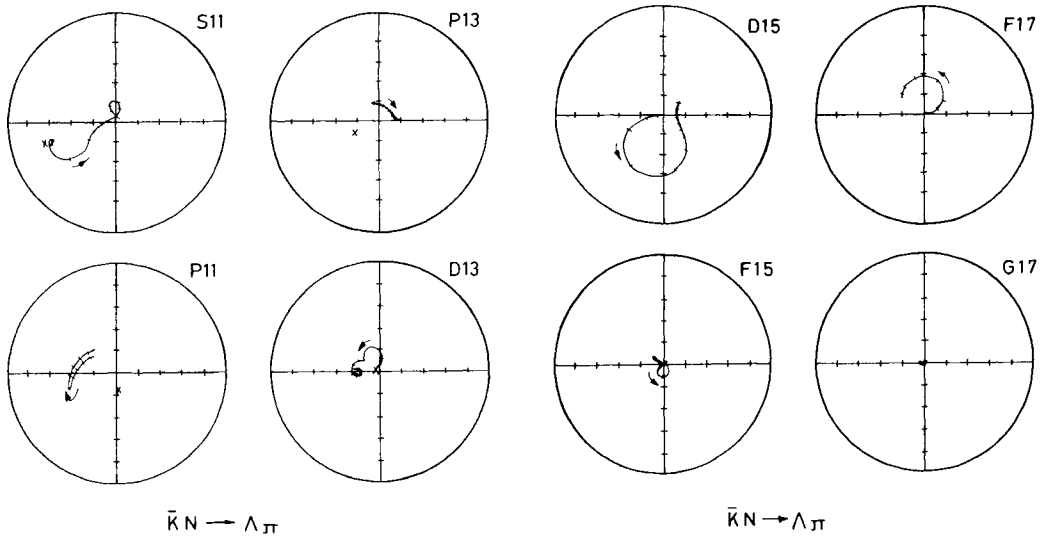

Fig. 27 s and p wave argand diagrams for the reaction $\bar{K}p \to \Lambda\pi$ from the analysis of Clayton et al. (351). The d waves and higher are very similar to those of Litchfield (1011). The crosses are the low energy solutions of Tripp.[21]

the $\bar{K}N$ channel, the d-wave and higher amplitudes are all in good agreement. The problem in the lower amplitudes seems to arise from two causes

(1) the presence of the two solutions found by Litchfield and previously by the energy independent analysis of the CHS collaboration[25];

(2) the lack of any phase constraint at low energies below the $\Sigma(1765)$.

It is clear from figures 25-27 that the solution of Clayton et al. is solution 2 of Litchfield. The fact that the energy dependent analysis chooses solution 2 is not surprising since it is less structured than solution 1. However if the choice of solution that can be made in the $\Sigma(1580)$ region is valid then this is a case where the least structured solution is <u>not</u> the valid one. The S and P waves of LMMO, fig 28, prefer solution 1 though above 1800 MeV there is some disagreement, possibly due to the divergence of their parameterisation at the end of the analysis range. Whether the preference of the multichannel analysis for solution 1 despite its greater complication indicates that the unitarity constraints prefer this solution is an important point that should be investigated as soon as possible. The analysis of Baillon agrees in the region of the unique solution but at low energies seems to suffer both from the lack of constraint on the phase and also in jumping between the two solutions. The low energy amplitudes of Tripp[21] are shown as the crosses in figure 27. The lack of any phase constraint in this channel means that the amplitudes can be rigidly rotated anywhere in the circle. They have been set so that the large s waves correspond. They do not agree well with any of the analyses but the analysis of Litchfield (1011) has shown that there are four Barrelet ambiguities that cannot be distinguished at these low energies in this channel alone.

New data on the reaction $K^-n \to \pi^-\Lambda$ in the centre of mass energy region 2050 to 2175 MeV is presented by Corden et al (1009).

At higher energies results are available from the College de France - Saclay energy dependent analysis in the energy region 2000-2400 MeV. The resonance parameters obtained are given in Table VII.

Amplitude	Reaction	Mass (MeV)	Width (MeV)	$\sqrt{xx'}$
P13	$\Lambda\pi$	2141	180	-0.19
P13	$\Sigma\pi$	not necessary		
D15	$\Lambda\pi$	2261	100	-0.12
D15 (or D13)	$\Sigma\pi$	2280	100	0.10
F05	$\Sigma\pi$	2150	150	0.04
F15	$\Lambda\pi$	not necessary		
F15	$\Sigma\pi$	2070	140	0.05
F17	$\Lambda\pi$	2030	170	-0.18
F17	$\Sigma\pi$	2030	150	-0.10
G07	$\Sigma\pi$	2120	160	0.14
G19	$\Lambda\pi$	2210	57	0.09
G19	$\Sigma\pi$	2210	60	0.04
H09	$\Sigma\pi$	2350	100	0.12

TABLE VII/ Resonance parameters from the College de France-Saclay analyses of the $\Lambda\pi$ and $\Sigma\pi$ channels between 2000 and 2400 MeV.

The reactions $\pi N \to K\Lambda$ and $\bar{K}N \to \pi\Lambda$ are related by crossing. Devenish et al. (115) have performed an interesting analysis in which they have fitted simultaneously the reactions $\pi^- p \to K^o \Lambda$ and $K^- p \to \pi^o \Lambda$ using the hypothesis of two component duality combined with fixed t dispersion relations. The duality hypothesis implies that the imaginary parts of the amplitudes are given entirely by the resonance contributions and from these the real parts may be calculated via the fixed t dispersion relations. In the analysis the masses and widths of the N* and Σ* resonances included were taken from the Particle Data Group compilation[29] and the variable parameters were their amplitudes at resonance. Despite the relatively small numbers of free parameters reasonable fits were obtained to all the data and the fitted values of the amplitudes at resonance in both channels were in good agreement with those found in the partial wave analyses. The success of this analysis not only substantiates the duality hypothesis but also implies that the present set of dominant resonances is sufficient to explain most of the features of the data.

Σπ Final States

The Σπ channel is much worse understood than either Λπ or $\bar{K}N$ mostly because of the inferior data. Ross et al. of the RHEL-IC collaboration, have presented an analysis in the energy range 1540-2170 MeV (349). Better parameters are obtained for the established resonances and indications of the resonances shown in Table V are found.

An interesting new source of Σπ data is the reaction

$$K_L^o p \to \Sigma^o \pi^+$$

Data is presented by Cho et al (105) in the region of 550 MeV/c. This channel is pure isotopic spin 1 and thus provides a good check of the isospin separation of the $K^- p$ analyses. Figure 29 shows the $\Sigma^o \pi^+$ differential cross section, averaged over the rather broad beam momentum region 450-600 MeV/c and the predictions of the analyses of Kim (K)[27], Armenteros et al.[28] (A) and Ross et al (R). Neither Kim nor Armenteros et al. provides a very inspiring fit to the data but Ross et al. fit quite well. As in the Λπ channel their amplitudes are completely different from those of Tripp in the low energy region.

Other Channels

Paper 559 of Jones presents an analysis of the reaction $K^- p \to \Sigma^o \eta$ near threshold. This reaction with two missing neutrals is clearly hard to isolate. Cross sections, shown in figure 30, and angular distributions are obtained but with limited statistics. The cross section bump can be fitted with either s or p wave scattering length or an s-wave resonance close to threshold. The resonance

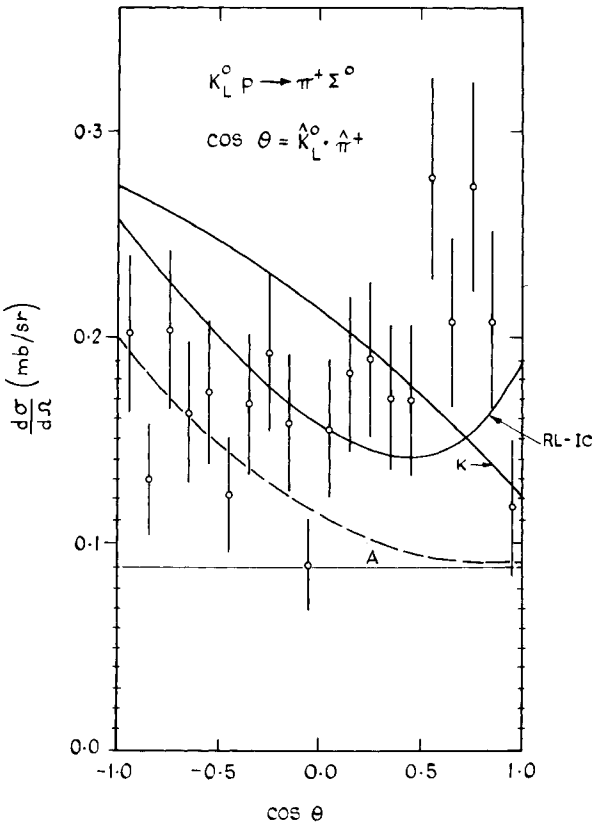

Fig. 29 Angular distribution for the reaction $K_L^o p \to \Sigma^o \Pi^+$ at 550 MeV/c from Cho et al. (105). The curves are the predictions for this reactions from the analyses of $K^- p \to \Sigma^{\mp} \pi^{\mp}$ by Kim [27] (K), Armenteros et al. [28] (A) and Ross et al. (349) (R).

is very slightly favoured and gives parameters consistent with those of the Σ(1740) observed in other channels[29]. Assuming the bump is a pure resonance yeilds a $\sqrt{xx'}$ at resonance of 0.23 ± 0.01 but this takes no account of any background and the systematic error to be added is clearly large.

Corden et al. present in paper 563 an analysis of the Λ(1520) observed in production in K^-d interactions. They observe the $\bar{K}N$, Σπ, Λππ, and Σππ decay modes and measure branching ratios of 44.8 ± 1.4%; 42.6 ± 1.4%; 9.1 ± 0.6%; 0.7 ± 0.2% respectively, all consistent with the PDG values. They have performed a Dalitz plot analysis of the reaction Λ(1520) → Λππ. They find that only the final states Σ(1385)π in an s-wave and Λε in a p wave are required (ε is the I = 0 s wave ππ phase shift). They find that their results depend strongly on the form they use for the ε phase shift. Using the same form as that used by Mast[30] in a formation study of this reaction they find very similar results ie. approximately 80% of the decay is Σ(1385)π. However using the phase shifts of Scharenguivel et al.[31] a Σ(1385)π fraction as low as 28% can be obtained. The Λε fraction stays rather constant but the interference term becomes very large.

Since the interference between a Breit Wigner and a constant background is very difficult to distinguish from a pure Breit Wigner this result is probably not very surprising, there is probably a strong correlation between the fractions. They conclude that 58 ± 22% of the decay goes via Σ(1385)π rather lower than the value of Mast et al but the error is clearly large.

Corden et al. (561) have also presented an isobar model analysis of the reactions

$$K^-n \to K^-\pi^-p$$
$$\to \bar{K}^o\pi^-n$$

Using a similar method to the Berkeley-SLAC analysis of ππN. The isobars required are Λ(1520), Λ(1815), Δ(1230), N(1520) and K^*(890). With very many fewer events than are available in the ππN analysis (a total of 16,000 for the two channels) and more isobars only a limited analysis determining the dominant partial waves in each isobar channel is possible. The cross sections for these amplitudes are shown in Fig. 31 for the $K^o\pi^-n$ channel and Fig. 32 for $K^-\pi^-p$. Generally $7/2^+$, $5/2^+$ and $3/2^+$ amplitudes dominate. Peaks can be seen in the region of the Σ(2030) in the $7/2^+$ amplitudes. They find $\sqrt{xx'}$ for the Σ(2030) resonance amplitude of 0.16 ± 0.02 in the Λ(1815) channel and upper limits at 0.17 and 0.15 respectively for K^*N and KΔ. These values are in good agreement with the results of Litchfield et al. who analysed the channel $K^-p \to K^-p\pi^o$ using a rather different method.[32]

The major difference between the analyses is that Corden et al. find no Λ(1520)π decay of the Σ(2030) whereas this process was found to be strong by Litchfield et al. The Λ(1520)π decay turns out to be more difficult to isolate than the other decay modes as the D wave decay gives strong contributions only to the low order moments of the angular and decay distributions unlike the ΔK and K^*N, decays where there are large contributions to the high order moments.
On the other hand Corden et al have a much cleaner channel in $K^-\pi^-p$ than Litchfield et al in $K^-p\pi^o$ A simultaneous analysis of all $\bar{K}N \to \bar{K}N$ π channels could help to sort out the differences. The strong Λ(1520)π decay of the Σ(2030) is something of an embarrassment to SU(3) since the Σ(2030) is predominately {10} and thus should not decay to an {8} and {1}. The decay must therefore be to the small {8} component of the Λ(1520) and a strong decay to its predominately {8} mixing partner the Λ(1690), would be expected but is not observed.

4) CURRENT STATUS OF RESONANCES

I have attempted to make a survey of the present

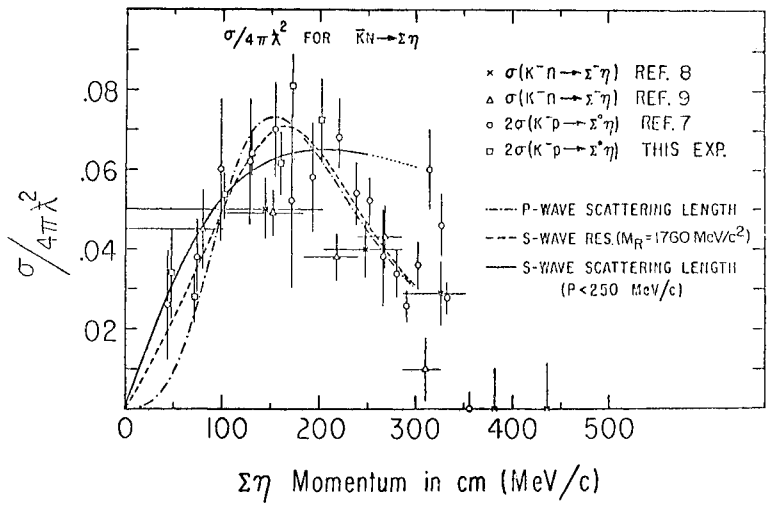

Fig. 30 Cross sections devided by $4\pi\lambda^{-2}$ for the reactions $\bar{K}N \to \Sigma\eta$ from Jones (559) and earlier work.

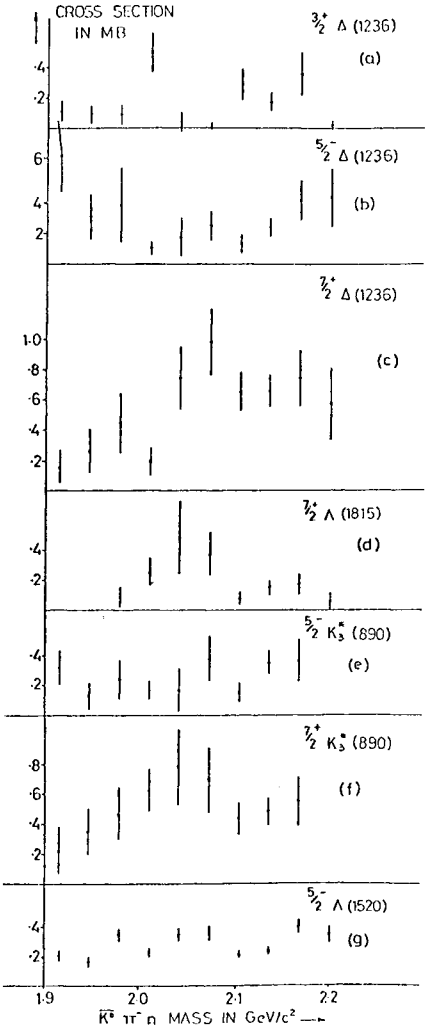

Fig. 31 Cross sections for the dominant isobar amplitudes in the reaction $\bar{K}n \to \bar{K}^0\pi^-n$ as a fraction of centre of mass energy from Corden et al. (561).

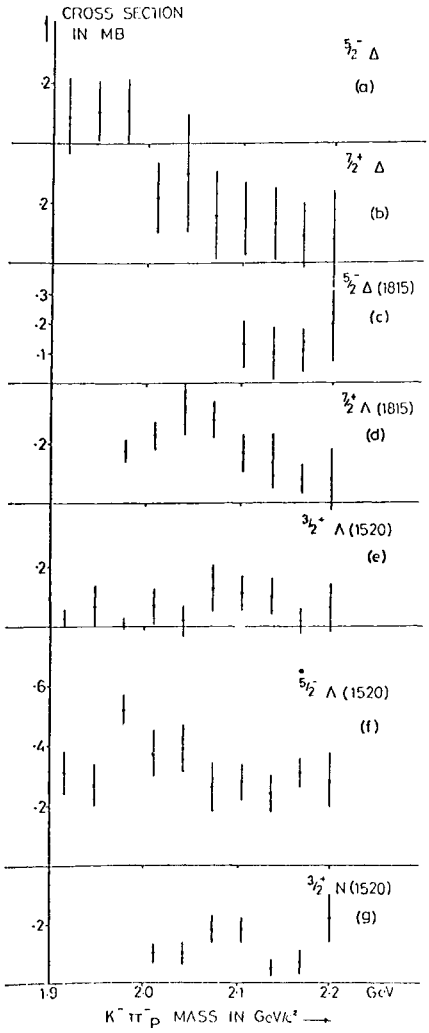

Fig. 32 Cross sections for the dominant isobar amplitudes in the reaction $\bar{K}n \to \bar{K}^-\pi^-p$ as a fraction of centre of mass energy from Corden et al. (561).

resonance candidates with a view to extracting a set of resonances that can be used to test classification schemes and models with some degree of reliability. I have adopted the star classification of the PDG, **** being a cast iron resonance down to * meaning a possible candidate. I have tried to only include those candidates that I estimate (as far as these things can be estimated) have at least a 50% chance of survival. However take warning that this implies that up to 50% of the * resonances could eventually disappear. This type of classification is obviously subjective and personal. In general I agree with the PDG classification but there are detailed differences. In particular I can reject states as being less than * while the PDG has to list them. For the N's and Δ's I have relied heavily on the analysis of Ayed and Barcyre since it seems that at least at high energies this analysis fits the charge exchange polarisation data which only became available after the analysis, while earlier analyses do not. It appears that in the πN channel the amplitudes are so well established that the latest analysis with the latest data probably gives the best representation of the amplitudes. I have however taken note of previous πN analysis and of course extra information is provided by the results of analyses of other channels $\pi\pi N$, ΛK, ΣK etc.

The $\bar{K}N$ amplitudes are considerably less well defined and a lot of art and/or personal predjudice still enters the analyses. I have in general adopted the criterion of rejecting unsubstantiated claims when an later analysis of the same channel using the same method has not seen the resonance. Of course some of these states may reappear in the future. I have also not included unsubstantiated resonances from the analysis of Langbein and Wagner [25] because of the much greater structure seen in their amplitudes than in other analyses which fit the data equally well and their known problems with the discontinuity of their Barrelet zeros [18] which probably causes this structure.

I shall not here give best parameters for masses widths and amplitudes at resonance as there are obviously even more difficult to be certain of than the existance or not of a state. I recommend anybody who wishes to find these parameters to take the PDG data listings and guess by eye a mean value and spread of the results for each parameter. This is as accurate as any other method. Parameters determined in this way have been used for $SU(6)_W$ fits to the resonances classified in the $\{70, 1^-\}$ and $\{56, 2^+\}$ multiplets(most of the reasonably well established resonances) and are tabulated in the mini-rapport of Hey.

Only strangeness 0 and -1 resonances are listed. Outside the ground state 1/2+ and 3/2+ multiplets no Ξ^* or Ω^* states have their spin parity even tentatively indicated, an absolute minimum for any sensible classification.

To avoid confusion I have in most cases called the resonance by the name listed in the current PDG compilation though the actual masses may be a considerable distance from the named mass. All star classifications are only accurate to ± one star.

**** Resonances (19 states)

Partial Wave	N*	Δ	Λ	Σ
S1 1/2 −	N(1535) N(1700)	Δ(1650)	Λ(1405) Λ(1670)	
P1 1/2 +	N(1470)			
P3 3/2 +		Δ(1232)		Σ(1385)
D3 3/2 −	N(1520)		Λ(1520) Λ(1690)	Σ(1670)
D5 5/2 −	N(1670)			Σ(1765)
F5 5/2 +	N(1688)		Λ(1815)	
F7 7/2 +		Δ(1940)		Σ(2030)
G7 7/2 −			Λ(2100)	

These resonances are strong enought to be used as anchor points in many partial wave analyses. Disagreement amongst analyses as to the exact parameters and branching fractures are almost certainly due to underestimation of errors. The general features of the resonances are well understood.

*** Resonances (12 states)

Partial Wave	N	Δ	Λ	Σ
S1 1/2 −				Σ(1750)
P1 1/2 +	N(1780)	Δ(1910)		
P3 3/2 +	N(1810)			
D3 3/2 −		Δ(1670)		Σ(1940)
D5 5/2 −			Λ(1830)	
F5 5/2 +		Δ(1890)		Σ(1915)
G7 7/2 −	N(2150)			
H9 9/2 +	N(2220)			
H11 11/2 +		Δ(2420)		

States with these quantum numbers and approximate masses certainly exist however analyses do not always agree on their masses, widths and amplitudes at resonance. We still have something to learn about these resonances.

** Resonances (12 states)

Partial Wave	N	Δ	Λ	Σ
P1 1/2 +			Λ(1750)	Σ(1620) Σ(1880)
P3 3/2 +			Λ(1860)	
D3 3/2 −	N(1700) N(2040)			Σ(1580)
D5 5/2 −		Δ(1960)		
F7 7/2 +	N(1990)		Λ(2100)	
G9 9/2 −				Σ(2250)
H9 9/2 +			Λ(2350)	

While looking good candidates these resonances require confirmation. Those states which appear in the total cross section (Σ(1580), Δ(1960), Σ(2250) and Λ(2350)) presumably exist but require confirmation of their spin parity. I would expect at least 90% of these resonances to survive.

* Resonances (16 states)

Partial Wave	N*	Δ	Λ	Σ
S1 1/2 +	N(2100)	Δ(1900)	Λ(1870)	Σ(2000)
P1 1/2 +				Σ(1770)
P3 3/2 +		Δ(1690)	Λ(1600)	Σ(1720)
		Δ(1900)		Σ(2080)
D5 5/2 −	N(2100)			Σ(2260)
F5 5/2 +	N(2000)		Λ(2120)	Σ(2150)
G9 9/2 −	N(2130)			

These are possibles but don't put your shirt on them. I would not be surprised to see 50% of them disappear in time. They have mostly either high mass or low spin and are thus hard to detect. They are seen only in one channel or with widely differing parameters. The Σ(1720), Σ(1770), Σ(2150), Σ(2260), Λ(1600) and Λ(2120) were first reported at this conference and thus obviously require confirmation. I have included rather tentatively two P3 Δ's. Ayed and Bareyre

mention only one state at 1900 MeV whereas the $\pi\pi N$ analysis of the SLAC-Berkeley groups (468) find one state at around 1650 MeV and this is confirmed by the Saclay analysis. The Almehed and Lovelace analysis[33] also found a state àt ≈ 1690 MeV. The Ayed and Bareyre amplitudes show some structure at around 1700 MeV and it is possible to imagine some structure at 1900 MeV in the $\pi\pi N$ Argand diagram. It should be kept in mind however that this is possibly only one state.

I do not consider that there is sufficient evidence for the following resonances, listed in the PDG complilation, to warrant considering them for classification purposes: P1 N(1532), G9 Δ(2170), D3 Λ(2010), S1 Σ(1620), P3 Σ(1840), G7 Σ(2100). Only states listed as probable in the RHEL-IC analyses have been considered if not previously reported. I have called the F7 Λ resonance the Λ(2100) rather than the Λ(2020) listed in the PDG tables because the effect seen in the elastic channel (350, 176) is almost certainly not the same as that claimed at a much lower mass in an unconfirmed $\Sigma\pi$ analysis [34] which also claimed the G7 Σ(2100) and had completely different parameters for the F7 Σ(2030) and G7 Λ(2100) from those which are now generally accepted.

5) SU(6) FOR BEGINNERS

Armed with the baryon states discussed above we can search for systematics amongst the baryon spectrum. The classification of the resonance states into SU(3) multiplets was a great step forward and nothing has since arisen to cast any doubts on this approximate symmetry . The search for a higher symmetry to combine the SU(3) multiplets has however had a chequered history. The low lying baryons fall rather pleasingly into multiplets of SU(6), e.g. the $\frac{1}{2}^+$ nucleon octet and $3/2^+$ decuplet making up a {56}. However application of the symmetry to decay rates immediately produced contradiction.[35] The first really successful application of a higher symmetry to baryon decay rates was by Faiman and Plane [36] who fitted the decay amplitudes of the low lying negative parity baryons using an, at the time, arbitrarily broken $SU(6)_W$ symmetry (1-broken $SU(6)_W$) in which the contradictions were removed by allowing separate coupling constants for the decays into the two allowed orbital angular momentum states of each supermultiplet instead of one overall coupling constant. In the last two years this empirical rule has been given some theoretical justification by the application of the Melosh transformation.[37] The paper of Hey et al (626) has repeated and extended the work of Faiman and Plane using the very large amount of data now available including the decays to $\Delta\pi$ and $\Sigma(1385)\pi$ which place very strong constraints on the model. They find that this form of $SU(6)_W$ fits the data nearly as well as SU(3) and indeed can be used to resolve the SU(3) assignments of states. Figure 33 shows the SU(3) coupling constants calculated from the $SU(6)_W$ model compared with those measured by analyses of the

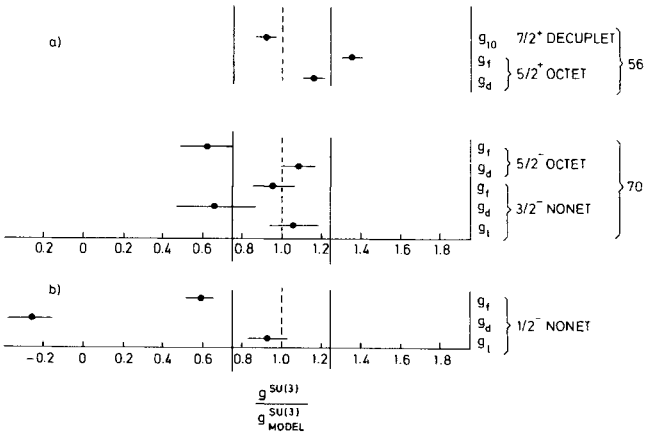

Fig. 33 Comparison of the $SU(6)_W$ predictions for the SU(3) coupling constants with the measured values for the SU(3) multiplets shown. Note the bad disagreement for the $\frac{1}{2}^-$ nonet probably due to the misassignment of states.

SU(3) multiplets. The agreement is very good apart from the $\frac{1}{2}^-$ nonet for which the detailed $SU(6)_W$ fit shows that there has been a misassignment of states. The quark model which, of course, explicitly includes SU(6) symmetry has also scored some notable successes and it now seems undeniable that $SU(6)_W$ symmetry is an underlying property of elementary particles.

Rosner (review paper in these proceedings) will discuss in detail the applications of these symmetries and models to the decay rates. Here I would like to discuss the assignment of the experimental states to the various $SU(6)_W$ multiplets and point to where experiment can provide new and crucial data.

Firstly for those who are not experts in the field, I will indicate how the SU(6) multiplets are built up. Under SU(3) the baryons are considered to be made up of quark triplets (p,n,λ quarks) but no account is taken of the spin $\frac{1}{2}$ nature of the quarks. Including this spin gives another degree of freedom and instead of being represented as {3}'s the quarks may be represented as {6}'s. Combining three quarks to make a baryon then yields.

$$\{6\} \times \{6\} \times \{6\} = \{56\} + \{70\} + \{70\} + \{20\}$$

The curious may check that the funny arithmetic works. Thus the baryons are expected to appear in multiplets of {56}, {70} or {20}. The multiplets decompose into their SU(3) and spin components as follows:

$$\{56\} = \{8, 2\} + \{10, 4\}$$

$$\{70\} = \{8, 4\} + \{10, 2\} + \{8, 2\} + \{1, 2\}$$

$$\{20\} = \{8, 2\} + \{1, 4\}$$

where the first figure is the SU(3) multiplet and the second 2S + 1 where S is the total quark spin. Thus the {56} is made up of SU(3) octets with total quark spin 1/2 and SU(3) decuplets with total quark spin 3/2

Since the spin of resonances can be greater than 3/2 we must have some orbital angular momenta between the quarks. We may form the symmetry SU(6) ⊗ O(3) and produce multiplets of the type $\{n, L^p\}$ where n is the SU(6) representation L is the total quark orbital angular momenta and p is the parity of the final state. Thus the muliplet $\{56, 2^+\}$ is made up of positive parity states and consists of SU(3) octets with total spin $\underline{L} + \underline{S}$ (i.e. of J^p $5/2^+$ and $3/2^+$) and SU(3) decuplets of J^p $7/2^+$, $5/2^+$, $3/2^+$, $1/2^+$.

It should be emphasised that SU(6) in itself makes no predictions as to which of the multiplets should be present in nature, only specific models, such as the harmonic oscillator quark model, make these predictions. Thus it is of interest to examine the data in a model independent way to determine which multiplets are present.

The stable baryons plus the $3/2^+$ decuplet fit well into a $\{56, 0^+\}$ multiplet. Since the orbital angular momentum is zero only the $\frac{1}{2}^+$ octet and $3/2^+$ decuplet are present. The low lying negative parity states make up a $\{70, 1^-\}$ multiplet. Figure 34 shows the states allocated to this

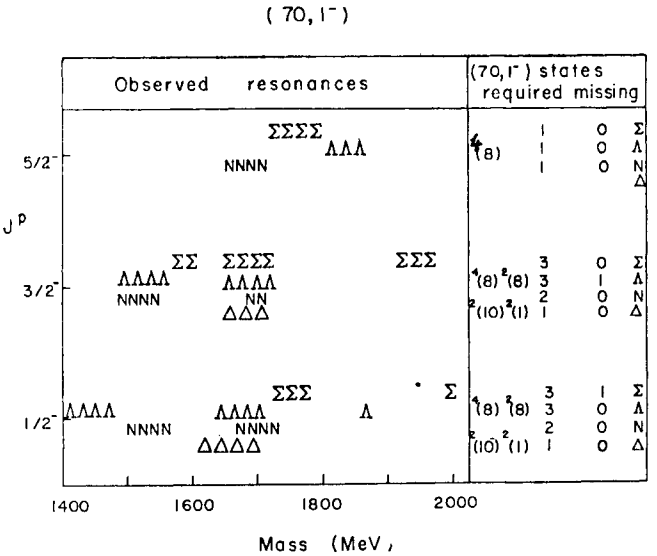

Fig. 34 Scatter plot of J^p against mass for states assigned to the $\{70,1^-\}$ $SU(6)_W$ supermultiplet.

multiplet plotted on a scatter plot of J^P against mass. N, Δ, Σ, Λ, have the obvious meanings and the number of symbols represents the status of the resonance. There are no negative parity states left unassigned below 1900 MeV. Recent confirmation of the $3/2^-$ N(1700) (465), $\frac{1}{2}^-$ Σ(2000) (349, 350, 351) and measurement of the spin parity of the $3/2^-$ Σ(1580) (522) have filled gaps in this multiplet which is now nearly complete, except of course for its Ξ and Ω members which I shall ignore throughout this section. Furthermore the detailed analysis of the decay rates of members of this multiplet (626) shows that they are described well by broken $SU(6)_W$ symmetry increasing our confidence that the states are correctly assigned.

In the mass region 1650 - 2000 MeV there is strong evidence for the existance of a {56, 2^+} multiplet. Here however we have to be more careful over assignments as there are positive parity resonances in this region that cannot belong to this multiplet.

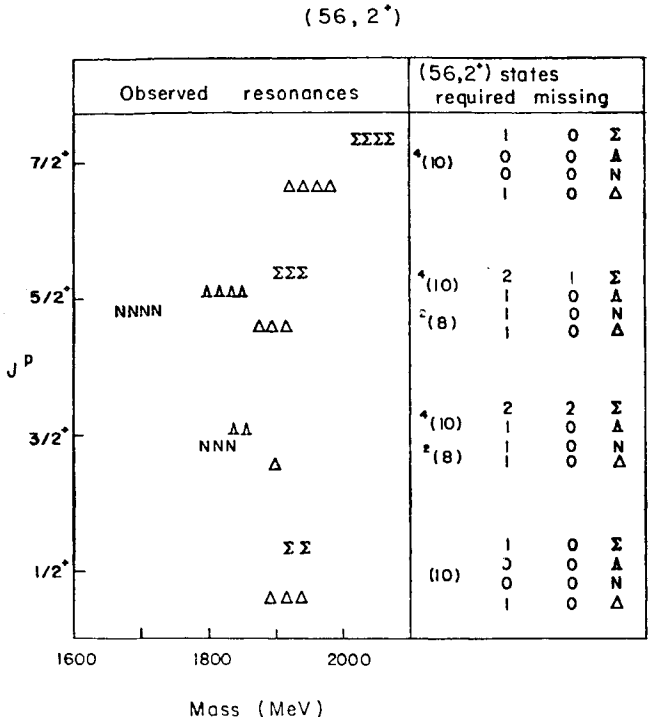

Fig. 35 Scatter plot of J^P against mass for states assigned to the {56,2^+} $SU(6)_W$ supermultiplet.

Tentatively we make the assignments shown in Figure 35 with, however, the proviso that some of the assignments could change when the other multiplets that have to be present are completed. Again the $SU(6)_W$ analysis of the decay rates works extremely well, even better than for the {70, 1^-}.

Having removed all those states from our experimental mass spectrum we may look to see what remains. Figure 36 shows the negative parity states. To the right are listed the SU(3) multiplets required to make up various SU(6) ⊗ O(3) multiplets. The following comments are in order.

(1) If all the states are taken at their face value at least two SU(6) multiplets are present.

(2) The $9/2^-$ N* can only be accommodated in the {70, 3^-}. The πN analysis of Ayed and Bareyre also claims a $9/2^-$ Δ resonance but the Argand diagram is unconvincing and I have not included it in the tables. If however it should be substantiated it would be strong evidence for the presence of a {56, 3^-}.

(3) The signs of the amplitudes at resonance of the Λ(2100) in the Σπ and Λπ channels require it to be a singlet state assuming the absence of strong

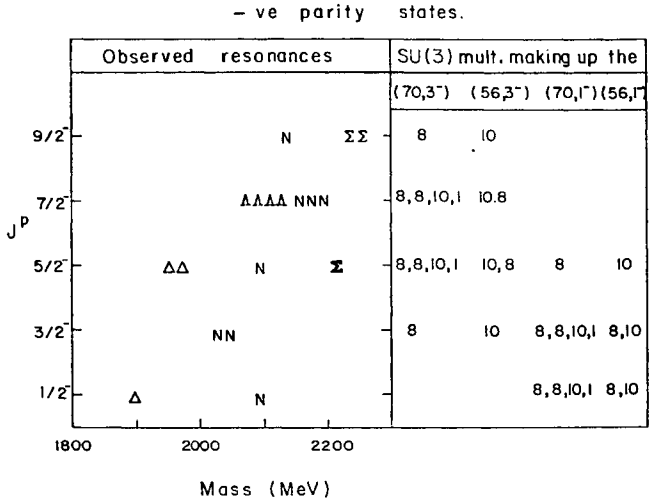

Fig. 36 Scatter plot of J^P against mass for the negative parity states which cannot be assigned to the lowest {70,1^-} multiplet.

mixing. It can thus only be a member of the $\{70, 3^-\}$ (4) The s-wave states must be members of the $\{70,1^-\}$ or $\{56, 1^-\}$. They could belong to the first radial excitation of the $\{70, 1^-\}$ in the quark model. However they are only * resonances and thus should be treated with some suspicion. If they are present they imply large numbers of other low spin resonances in this region and give our first indication of one of the major problems of practically all resonance models; far from being too many resonance states there are in fact far too few. However if for the moment we ignore the s-wave states the remainder fit rather well into the $\{70, 3^-\}$ with the $\{56, 3^-\}$ being rather strongly disfavoured.

The second comment highlights the already mentioned possibility of determining the SU(6) structure of the higher lying multiplets without doing complete partial wave analyses which are probably impossible above 2500 MeV. The spin parity of the highest lying states could however hopefully be determined by the structure in the highest Legendre coefficients of the expansions of the angular distributions. Figure 36 shows that the highest spin multiplet of the {56}is a{10} whilst that of the {70} is an {8}. Thus by studying the structure of the high spin Δ's and N*'s or Λ's one could hope to be able to determine approximately the positions of the {56}'s and {70}'s.

Positive parity states

The remaining positive parity states (Figure 37) clearly show two groupings, one corresponding to high mass, high spin and the other low mass, low spin. Considering the high spin states first, the $11/2^+$ Δ clearly requires the presence of a $\{56, 4^+\}$. The $9/2^+$ and $7/2^+$ nucleon and Λ states would also fall naturally into this multiplet though the mass range would then be slightly larger than that of the $\{56, 2+\}$. If the approximate mass degeneracy of the Δ states is repeated here they would all lie in the 2400 MeV region and would be unlikely to have been seen in the present partial wave analyses.

In the low mass region the Roper resonance seems at last to be gaining respectability. There are now also Σ and Δ candidates ($\Sigma(1660)$ and $\Lambda(1600)$) to complete its SU(3) octet. The signs of the $\pi\Delta$ decay amplitudes of the P11 N(1470) and P33 Δ(1690) show unambiguously that they have to be members of a $\{56, 0^+\}$ and the P13 $\Sigma(1720)$ is a good candidate to fill the remaining $S = -1$ slot in this multiplet.

The $\Delta\pi$ sign of the P11 N(1780) is the same as that of the N(1470) indicating that it too belongs to a $\{56, 0^+\}$. Possible Σ and Λ partners are also available. The indications are that this is therefore the second radial excitation of the ground state $\{56, 0^+\}$ and would indicate an approximate equal spacing rule for radial excitations.

If these assignments are all valid then in this energy region there are two $\{56, 0^+\}$ and one $\{56, 2^+\}$ multiplets. Thus there have to be 4 $3/2^+$ Σ's, 3 $3/2^+$ Δ's

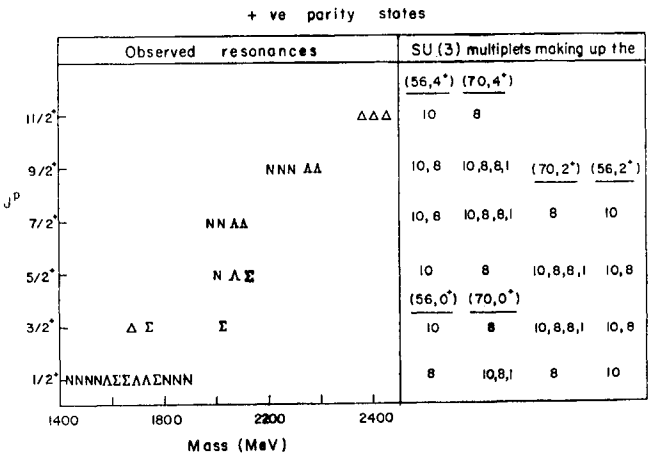

Fig. 37 Scatter plot of J^P against mass for the positive parity states that cannot be assigned to the lowest $\{56,0^+\}$ or $\{56,2^+\}$ multiplets.

and 3 $1/2^+$ Σ's present. Three $1/2^+$ states are observed in the preferred solution of paper 1011 analysing the $\Lambda\pi$ channel. All three however have negative amplitudes at resonance. The two states from the $\{56, 0^+\}$ are expected to have negative signs (Figure 38 taken from the review of Rosner [35] gives a table from which the resonance signs can be calculated given the F/D ratios of the multiplets) but the $\{56, 2^+\}$ Σ must have a positive sign as it is a decuplet member. The assignment of the $\Sigma(1880)$ to the $\{56, 2^+\}$ is thus dependent on there being sufficient intermultiplet mixing amongst these closely spaced states to change the sign of this amplitude. The negative sign of the $\Lambda\pi$ decay of the $\Sigma(2080)$ also implies that in the absence of mixing it cannot be a decuplet state but it could be assigned as the octet member of the $\{56, 2^+\}$ though its mass is rather high.

There remains only the $5/2^+$ N(2100), $\Lambda(2170)$ and $\Sigma(2150)$ possibly forming an SU(3) octet. These are only * resonances and therefore should not be taken too seriously but they could be assigned to $\{70, 4^+\}$, $\{70, 2^+\}$ or $\{56, 2^+\}$. It is amusing to note that the N* mass is approximatelythe same distance above the N(1680) as the Roper is above the nucleon and thus they could be the first members of the radial excitation of the $\{56, 2^+\}$. However the resonance signs of the Y*'s would classify then in a $\{70\}$ rather than a $\{56\}$.

A very interesting question in terms of the harmonic oscillator quark model is whether there is any evidence for the existance of the $\{70, 2^+\}$ multiplet which it predicts to be approximately mass degenerate with the $\{56, 2^+\}$. [38] Various arguments have been put forward in the past to show the existance of this multiplet and they are summarised below :

(1) The presence of the $7/2^+$ N* and Λ between 2000 and 2150 MeV cannot be accommodated in the $\{56, 2^+\}$.

(2) The absence of the p wave decay of the F_{35} $\Delta(1890)$ [39] was taken to imply mixing of the $\{56, 2^+\}$ with the $\{70, 2^+\}$.

(3) The signs of the high mass $5/2^+$ Σ and Λ mentioned above indicate their assignment to a $\{70\}$.

These points may be answered as follows:

(1) As shown above the $7/2^+$ resonances can naturally be placed in a $\{56, 4^+\}$ which is required to be present by the $9/2^+$ and $11/2^+$ resonances.

(2) The $SU(6)_W$ fit of Hey et al (626) predicts p and f wave amplitudes of the F_{35} which are approximately the same and equal to 0.09 compared with the measured values of 0.17 ± 0.06 for the f wave and

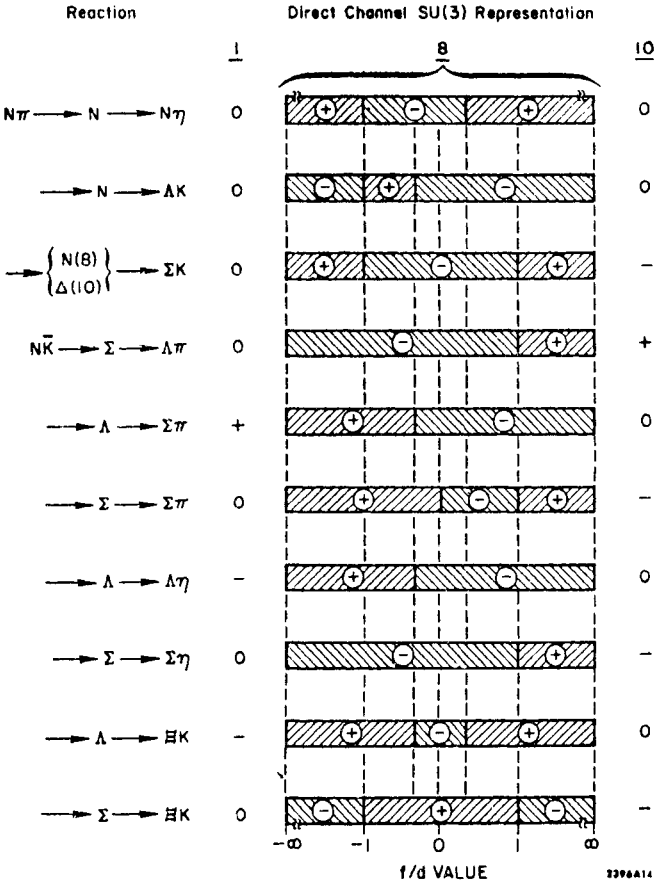

Fig. 38 Signs of resonant amplitudes in $\frac{1}{2}^+0^- \to \frac{1}{2}^+0^-$ reactions taken from the review of Rosner [38]. The baryon first convention is used. For octet states the sign depends on the F/D ratio. $SU(6)_W$ predicts F/D ratios of +2/3 for states in a $\{56\}$, -1/3 for states in a $\{70\}$ with quark spin 3/2 and +5/3 for $\{70\}$ state with quark spin $\frac{1}{2}$.

0.0 ± 0.06 for the p wave. They are thus both only 1.5 standard deviations from the predicted values.

(3) Large numbers of high spin resonances are required to fill the $\{70, 2^+\}$ which have not been observed. For example 3 new $5/2^+$ Σ's, 3 $5/2^+$ Λ's a $5/2^+$ N* and a $5/2^+$ Δ are required. In this region these high spin states are relatively easily observed, for example the $5/2^+$ $\Sigma(1915)$ is clearly seen although it has a very small elasticity. If we take the $7/2^+$ states to be members of the $\{70, 2^+\}$ and follow the usual rule that the highest spin states tend to have the highest mass then we expect all these $5/2^+$ states to lie below 2000 MeV where they have not been observed. This is a very good example of the constraint that SU(6) can now apply to resonance claims. If new states are claimed which have to start a new multiplet a very good explanation is required of why all the other states have not been seen. All this clearly does not rule out a higher lying $\{70, 2^+\}$, if the $5/2^+$ states are lowest lying states of a $\{70, 2^+\}$ with mean mass around 2300 then their partners would probably not yet have been found.

(4) Another contraindication of a low lying $\{70, 2^+\}$ is given by the $SU(6)_W$ fit of Hey et al (626) which assumed a pure $\{56, 2^+\}$ with no mixing and obtained a very good χ^2. The presence of the $\{70, 2^+\}$ would mean that not only the F35 but all the other states could be strongly mixed and the success of the simple fit would be very surprising.

To sum up I would consider that far from there being any evidence for a low lying $\{70, 2^+\}$ there is considerable evidence against its existance at least at the low masses required by the harmonic oscillator quark model[38].

There are now the following well established SU(6) ⊗ O(3) multiplets

$\{56, 0^+\}$	$\{70, 1^-\}$
$\{56, 0^+\}$ n=2	$\{70, 3^-\}$
$\{56, 2^+\}$	
$\{56, 4+\}$	

with possible indications of a third $\{56, 0^+\}$, a second $\{70, 1^-\}$ and either a second $\{56, 2^+\}$ or a $\{70, 2^+\}$. There is an indication of approximately equal mass spacings for the radial excitations. Below 2100 MeV the simple scheme of +ve parity {56}'s and -ve parity {70}'s seems to hold experimentally. There is no strong evidence as yet for either a $\{70, 0^+\}$ or $\{70, 2^+\}$ in this region. This is some embarrassment for the simple quark model[38] which requires positive parity {70}'s at least at the L = 2 level.

The search for the members of these positive parity {70}'s is the crucial experimental question of baryon spectroscopy at this moment. Their existence could be established either by observation of extra states that cannot be accommodated in the established multiplets, e.g. a second $7/2^+$ N^* or Λ, or by determining that the signs at resonance of any of the possible candidates is only appropriate to a {70}.

I would like to thank my scientific secretaries, Peter Kalmus and Brian Martin for their help in preparing this review and Tony Hey, Jaques Weyers and Jon Rosner for helpful discussions on the SU(6) classification.

REFERENCES

(1) R C Miller et al. Nucl. Phys. B37(1972) 401. R E Cutkosky and J C Sandusky; Phys. Rev. D9(1974) 2189.

(2) C Lovelace; Proceedings of the 1972 High Energy Physics Conference, Batavia, p.73.

(3) R Ayed and P Bareyre; Paper submitted to the IInd Aix-en Provence International Conference (1973).

(4) J W Alcock and W N Cottingham; Nucl. Phys. B56(1973) 301.

(5) G W London; Phys. Rev. D9(1974) 1569.

(6) G Giacomelli, P Lugaresi-Serra, G Mandrioli, A Minguzzi-Ranzi, A M Rossi, F Griffiths, A A Hirata, I S Hughes, R Jennings, B C Wilson, G Ciapetti, G Mastrantonio, A Nappi, D Zanello, G Alberi, E Castelli, P Poropat and M. Sessa; Nucl. Phys. B71(1974) 138.

(7) V J Stenger et al. Phys. Rev. 134B(1964) 1111.

(8) A K Ray et al. Phys. Rev. 183(1969) 1183.

(9) Tel. Aviv, Heidelberg collaboration, private communication from G Alexander and I Bar-Nir.

(10) Bologna-Glasgow-Edinburgh-Pisa-RHEL collaboration private communication.

(11) A A Hirata, G Goldhaber, B H Hall, V H Seeger, G H Trilling and C G Wohl; UCRL-20243 Jan. 1971. W E Slater, D H Stork, H K Ticho, W Lee, W Chinowsky, G Goldhaber, S Goldhaver and T A O'Halloran; Phys. Rev. Lett. 7(1961) 378.

(12) J S Ball, R R Campbell, P S Lee and G L Shaw; Phys. Rev. Lett. 28(1972) 1143.

(13) A Keman, S Y Fung, U Mehtani, Y Williamson, W Michael, G E Kalmus and R W Birge; "Baryon Resonances-73," proceedings of the Purdue Conference p.113.

(14) M S Milgram et al. Nucl. Phys. B18(1970) 1.

(15) P J Davies et al. Nucl. Phys. B44(1972) 344.

(16) A Brandstetter et al. Nucl. Phys. B39(1972) 13.

(17) W Langbein and F Wagner; Nucl. Phys. B53(1973) 251

(18) P J Litchfield; "S≤ - 1 Baryon Spectroscopy" proceedings of the IInd Aix-en-Provence Conference on High Energy Physics p.227

(19) P J Litchfield, T C Bacon, I Butterworth, J R Smith, E Lesquoy, R Strub, A Berthon, J Vrana, J Meyer, E Pauli, B Tallini and J Zatz; Nucl. Phys. B30(1971) 125.

(20) R Armenteros, P Baillon, C Bricman, M Ferro-Luzzi D E Plane, N Schmitz, E Burkhardt, H Filthuth, E Kluge, H Oberlack, R R Ross, R Bartloutaud, P Granet, J Meyer, J P Porte, J Prevost; Nucl. Phys. B8(1968) 195.

(21) R D Tripp; "Hyperon Resonances-70" Proceedings of the 1970 Duke Conference p.95.

(22) K K Li; "Baryon Resonances-73". Proceedings of the 1973 Perdue Conference p.283.

(23) A J Van Horn; LBL-1370(1972) (Thesis).

(24) A T Lea, B R Martin, R G Moorhouse and G C Oades; Nucl. Phys. B56(1973) 77.

(25) R Armenteros et al. Nucl. Phys. B8(1968) 183; P Baillon, paper presented to the IInd Aix-en-Provence Conference on Elementary Particle physics

(26) W Langbein and F Wagner; Nucl. Phys. B47(1972)477

(27) J K Kim; Phys. Rev. Lett. 27(1971) 356 and proceedings of the 1970 Duke Conference p.161.

(28) R Armenteros et al. Nucl. Phys. B8(1968) 223.

(29) Particle Data Group, Review of Particle Properties Phys. Lett. 50B(1974) 1.

(30) T S Mast et al. Phys. Rev. D7(1973) 5.

(31) Scharenguivel et al. Nucl. Phys. B22(1970) 16.

(32) P J Litchfield et al. Nucl. Phys. B74(1974) 12.

(33) S Almehed and C Lovelace; Nucl. Phys. B40(1972) 157.

(34) A Barbaro-Galtieri "Hyperon Resonances-70", Proceedings of the 1970 Duke Conference.

(35) For an simple review of the origins and basis of $SU(6)_W$ see J L Rosner SLAC-PUB-1391.

(36) D Faiman and D E Plane; Nucl. Phys. B50(1972) 379

(37) H J Melosh; Phys. Rev. D9(1974) 1095.

(38) R Horgan; Univ. of Oxford preprint 60-73.

(39) D Faiman, J L Rosner and J Weyers; Nucl. Phys. B57(1973) 45.